CHAPTER 4:

AUTOMATICITY OF VOICE CROSSMODAL PLASTICITY

Introduction

As detailed in Chapter 1, participants trained to interpret sensory substitution (SS) sounds have crossmodal plasticity generating visual activation in response to SS sounds (Amedi, et al., 2007; Arno, et al., 2001; Kupers, et al., 2010; Merabet, et al., 2009; Poirier, De Volder, Tranduy, et al., 2007; Poirier, De Volder, & Scheiber, 2007; Poirier, De Volder, et al., 2006; Ptito, et al., 2005; Renier, Collignon, Poirier, Tranduy, Vanlierde, Bol, Veraart, & Devolder, 2005; Renier & De Volder, 2010). The vOICe and SS in general have many of the characteristics of vision such as depth illusions, recognition, localization, and processing of SS stimuli in early visual areas. Nevertheless, unlike vision, vOICe interpretation is slow and laborious even after extensive training, and therefore is often assumed to be processed top-down (involves cognition). In contrast to vOICe, vision is often perceptual and passive (*i.e.,* automatically occurs without top-down attention) (detailed in Chapter 1, p. 53-55). Since vOICe is similar to vision in so many areas of perceptual processing, is there a component of neural vOICe processing that is perceptual just like vision? This chapter will investigate whether participants can crossmodally activate the visual cortex with vOICe automatically (without attention), in a similar fashion to perceptual visual processing.

Four functional Magnetic Resonance Imaging (fMRI) tasks will test the hypothesis that vOICe can activate visual cortex without attention. The first task is a passive listening task, where participants detect a pause in the vOICe sound that encodes a white noise image. The second task is an attention distraction task, where participants count backwards in sevens while a vOICe sound is played. The presence or absence of crossmodal plasticity (*i.e.,* visual activation) in each of these tasks will indicate whether vOICe can be processed in visual regions automatically after vOICe training in comparison to before training. We also tested the specificity of this crossmodal plasticity with a passive listening task for two familiar sounds: a beach sound (as an example of natural sound) and a Star Trek sound (as an example of artificial but familiar sound; task 3). If participants activate visual regions in response to familiar sounds when post-training scans are compared to pre-training scans, it will indicate that the crossmodal plasticity to vOICe is general, not specific to only vOICe sounds, and at least partly automatic. Finally, participants performed a visual control of the first task (passive listening to vOICe), while they detected a pause in the presentation of a white noise image (task 4). This is meant as a direct comparison between the visual response to white noise image and the visual response to the vOICe sound of a white noise image.

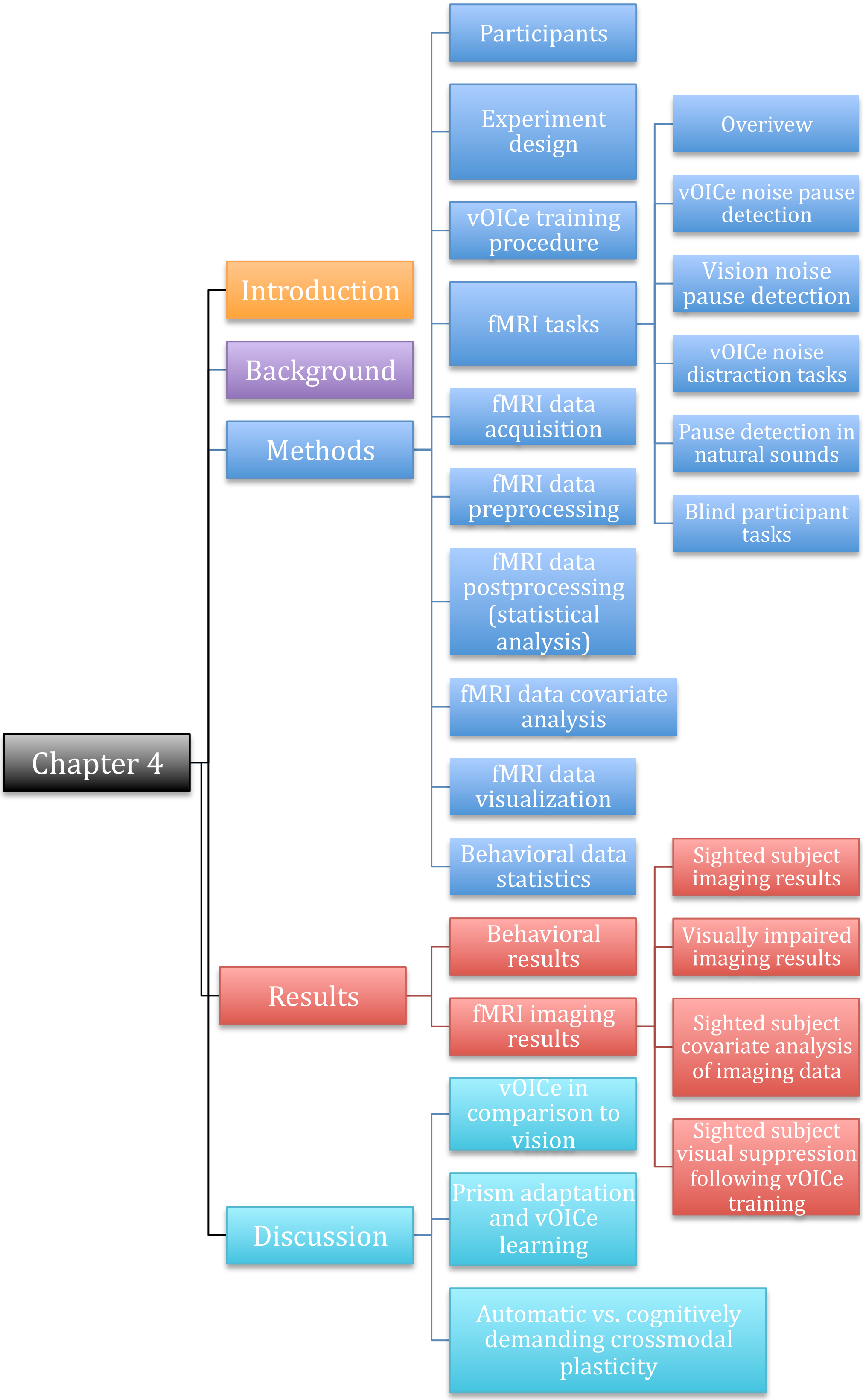
Chapter 4
Introduction
Background
Methods
Participants
Experiment design
vOICe training procedure
fMRI tasks
Overivew
vOICe noise pause detection
Vision noise pause detection
vOICe noise distraction tasks
Pause detection in natural sounds
Blind participant tasks
fMRI data acquisition
fMRI data preprocessing
fMRI data postprocessing (statistical analysis)
fMRI data covariate analysis
fMRI data visualization
Behavioral data statistics
Results
Behavioral results
fMRI imaging results
Sighted subject imaging results
Visually impaired imaging results
Sighted subject covariate analysis of imaging data
Sighted subject visual suppression following vOICe training
Discussion
vOICe in comparison to vision
Prism adaptation and vOICe learning
Automatic vs. cognitively demanding crossmodal plasticity

Figure 4.01. Outline of Chapter 4. This figure details the sections of Chapter 4 and their hierarchical structure.

Background

Neural imaging of sensory substitution users has shown crossmodal plasticity in blind and sighted trained users of SS, as discussed in Chapter 1. Studies using functional Magnetic Resonance Imaging (fMRI) have shown visual activation in response to sensory substitution (auditory or tactile) stimuli following training on these devices in blindfolded sighted and blind participants. In particular, imaging studies using pattern recognition and localization tasks with auditory sensory substitution have shown activation in early visual regions such as Brodmann Area (BA) 17 (so-called V1, or the primary visual cortex), BA 18, and BA 19 in blind and blindfolded sighted users (Poirier, De Volder, & Scheiber, 2007).

Surprisingly, despite fairly short training on sensory substitution devices (about 1 to 5 hours) for imaging studies, the crossmodal activation in visual regions seems to be robust. Experiments by Amedi and colleagues and Plaza and collaborators, have shown a functional or task-related activation of visual regions (Amedi, et al., 2007; Plaza, et al., 2009). Further, repetitive Transcranial Magnetic Stimulation (rTMS) studies have indicated that there is a causal relationship between sensory substitution performance and neural activation in visual regions for late and early blind (Collignon, et al., 2007; Merabet, et al., 2009). This may possibly indicate the “metamodal” nature of the visual cortical processing (Pascual-Leone & Hamilton, 2001) (see Chapter 1). Additional background detail on sensory substitution imaging studies can be found in Chapter 1.

Behavioral automaticity studies have been discussed in detail in Chapter 1 and Chapter 3. In general, there are several different criteria for automaticity, including:

“Goal independence criterion,” “the non-conscious criterion,” “speed criterion,” and attentional load sensitivity (Spence & Deroy, 2013). These criteria have been tested with a range of techniques on several different elements of perceptual processing (see Chapter 3 p. 91-92). Many types of visual tasks such as visual search and face perception have been shown to meet some automaticity requirements (see Chapter 1 p. 53-55). As was highlighted in Chapter 3 (p. 91-92), distraction tasks have been used for many multisensory behavioral tests of automaticity (*i.e.,* testing attentional load sensitivity). In particular, in Chapter 3 (p. 95-96), a distraction paradigm was discussed to test the attentional load criteria of automaticity for interpreting vOICe sounds. In the task, participants counted backwards in sevens or performed a visual search task while the vOICe sound was played, and then matched the vOICe sound to one of three images displayed (Chapter 3). It was found that the distraction tasks did not significantly diminish the participants’ ability to match vOICe sounds with images. Therefore, the Chapter 3 experiment indicated that vOICe interpretation can be automatic.

Automaticity studies in the literature have also investigated whether visual neural processing and thereby visual neural activation is independent of attention. As detailed in Chapter 1 (p. 54-55), ignored visual stimuli activation intensity is modulated by attentional load to an alternative task. However, the neural processing of ignored visual stimuli is not eliminated by high attentional load to another visual task. Therefore, the processing of visual stimuli is automatic, but the intensity of that processing may vary with attention. A similar distraction paradigm will be used in this Chapter to test whether attentional load reduces or eliminates the processing of vOICe sounds in visual brain regions.

One challenge to fMRI investigations with sensory substitution is the visualization, or the mental-visual imagery of stimuli by the sighted users of vOICe. Visualization occurs when a short-term memory is spatially re-imagined without direct visual input (Kosslyn & Thompson, 2003). Visual imagery can activate visual cortex, and that activation is retinotopic (activating neighboring neural regions for adjacent regions of visual space) (Klein et al., 2004; Slotnick, Thompson, & Kosslyn, 2005). In a meta-analysis of visualization literature, Kosslyn and Thompson found that several individual conditions significantly correlated with early visual activation during visualization in PET, single photon emission computed tomography (SPECT) and fMRI studies. A few conditions listed by Kosslyn and Thompson included a main task identifying high-resolution image details, a baseline task that is not resting state, a main task testing visual shape properties (not spatial visual properties), a main task lasting 5 minutes or less, or a sensitive neural scanning technique (*i.e.,* 3T or 4T fMRI) (Kosslyn & Thompson, 2003). Visual activation has been shown to occur during a rest or baseline task (with eyes closed) (Kosslyn, Thompson, Klm, & Alpert, 1995). This is likely the reason that studies with a resting baseline and a visualization main task result in visual activation in higher-level visual cortices but not in V1 or V2 (*i.e.,* early visual activation is subtracted out by the baseline). It has also been found that visual-imagery neural activation from short-term memory is stronger than imagery activation from long-term memory (Kosslyn & Thompson, 2003). Interestingly, as mentioned above, visual spatial reasoning, despite often using visualization, does not activate visual cortex, especially when it is not shape-based (Kosslyn & Thompson, 2003).

Visual activation due to visualization has been shown to be causally linked to the visualization task performance. Kosslyn *et al.* used repetitive Transcranial Magnetic Stimulation (rTMS) to deactivate the calcarine cortex (BA 17) prior to performing a visualization task (Kosslyn et al., 1999). Both the performance of the visualization task was reduced and the performance time (the time to task completion) was prolonged when rTMS was applied to BA 17 in comparison to directed away from BA 17. Further, Farah, Soso and Dasheiff showed in a case study that the "visual angle of the minds eye" was reduced in half horizontally but not vertically when one hemisphere of the occipital lobe was surgically removed from a patient (Farah, Soso, & Dasheiff, 1992). This reduction in size is expected based on the topographical mapping of the left visual field to the right visual cortex, and vice versa. In contrast, there are studies that indicate patients with widespread early visual region damage can often still visualize images. These studies may be an indication of long-term, functional re-organization within the damaged brain, and therefore not negate the necessity of early visual activation for visualization within the normal brain (Kosslyn & Thompson, 2003).

Studies of mental imagery in the blind (late and early onset) have indicated that they can produce, integrate, and manipulate mental images amalgamated from past experience and remaining sensory experience (Cattaneo & Vecchi, 2011). The early blind participant studies have focused on the imagery of tactile shapes and objects. Tactile imagery activated the occipital cortex in early blind participants for "visualization," or perceptual imagery from shape rotation, tactile texture, and auditory stimuli (Kaski, 2002; Lambert, Sampaio, Mauss, & Scheiber, 2004; Rosler, Roder, Heil, & Hennighausen, 1993; Uhl et al., 1994). In Lambert *et al.*'s study, the name of an animal was listed, and the early blind participants were asked to create a mental image of that animal. The early blind fMRI data contained neural activation in response to animal imagery including BA 17, BA 18, and BA 19 (with a region of interested analysis). Overall, it seems that the early and late blind can have perceptual imagery that is based on tactile perception and long term memory. In contrast, visualization by sighted individuals relies more heavily on visual spatial information.

The importance of visualization to visual activation by sensory substitution is still under active debate. Poirier *et al.* (2007) argues that visualization is the main method of SS visual activation in sighted sensory substitution users, and crossmodal plasticity is the main method for early blind users (Poirier, De Volder, & Scheiber, 2007). In contrast, fMRI studies using sensory substitution argue that the early blind participants have quite similar imaging results to the sighted participants, and therefore likely used a similar crossmodal method. Since the early blind can't visualize in the same way that the sighted can, never having vision, it not likely that image visualization played an important role in the visual activation from sensory substitution (Amedi, et al., 2007). Other methods used for controlling for visual imagery include additional control participants (not trained on sensory substitution) and auditory (non-sensory-substitution) tasks (Amedi, et al., 2007). Occasionally, a separate visual imagery control task relevant to the main experiment is also used (Merabet, et al., 2009).

Since our fMRI experiments were designed to identify early visual-cortical activation due to vOICe training, a similar possible activation pattern due to visualization is of critical concern. Thus, we designed fMRI scanning experiments with (a) a distraction task, (b) white noise stimuli, (c) early blind participants, and (d) a post-experiment questionnaire on visualization, to address this difficult visualization issue.

We describe the visualization issue as “difficult” because it is very challenging to systematically avoid visualization. Worse than that, more efficient visualization via SS training may not be just an artifact, but rather an intriguing element of the underlying neural mechanisms generating the performance improvement. Utilizing these manipulations (a)-(d) above, we may obtain some indications as to how visualization or other strategies are employed in sighted and blind participants similarly or differently.

Methods

Participants

Ten sighted participants were recruited from the Caltech community (2 Female and 8 Male). All fMRI and behavioral experiments were approved by the Caltech Internal Review Board. All participants had not been trained previously on a sensory substitution device.

One severe low-vision participant (visual acuity: 20/420, Male) and 3 blind participants were recruited from the local blind community (1 Female, 2 Male). The blind individuals were two congenitally blind (WB and SB: Retinopathy of Prematurity, entirely blind since infant) and 1 late blind (Retinitis Pigmentosa, light-perception, 30 years of blindness). The late blind participant had a hearing impairment, and wore a hearing aid. The hearing aid was used during vOICe training, but removed during the fMRI scans; the audio volume was increased during fMRI scanning to compensate. The second congenitally blind (SB) also had a minor hearing impairment in one ear, but did not require a hearing aid. All fMRI and behavioral experiments were approved by the Caltech Internal Review Board for blind participation. The visually-impaired participants had not been trained previously on a sensory substitution device.

Experiment Design

This fMRI experiment has a scan session before vOICe training, followed by vOICe training, and then a scan session following vOICe training, all occurring within two weeks (Figure 4.02). The two scan sessions contain the same tasks in order to capture the participant's neural processing difference due to the training between the scan sessions. The vOICe training lasts for four consecutive days (about one hour per day), and in addition, a short vOICe training session occurs directly before the final scan session, which lasts only 30 minutes. The fMRI scan sessions last two hours each, including experiment setup and audio testing. One participant performed all tasks before and after vOICe training (all comparisons are within subject comparisons).

vOICe Training Procedure

Participants used a vOICe device during auditory sensory substitution training. A detailed description of the vOICe device and general procedures is listed in Chapter 2's methods (p. 63-64).

vOICe device training lasted for about five hours between the pre-training and post-training fMRI scanning sessions. Training was performed for about an hour per day for four days, and a final session on the fifth day of about 30 minutes. Training was performed at a black-felt-covered table, or at a black-felt-covered wall (Figure 4.03 shows the black-felt-covered table). Training sessions began each day with a localization evaluation task, and then continued with localization and recognition training exercises.

The localization task assessed the participant's progress in learning the vOICe translation algorithm and their ability to localize objects with the vOICe device (Figure

4.03 shows task setup). The localization task was performed at the black-felt-covered table. The trainer would place a white circle in one of five locations on a black felt board, and the participant would locate the circle with vOICe, center the circle in the field of view, and then reach for the circle with one finger. The distance between the participant's reach and the circle's center would be measured as a metric of inaccuracy. Feedback was provided to participants by moving their finger from the reached position to the center of the white circle. Thus, the correct direction and location of the circle was provided through tactile and proprioceptive feedback.

The training tasks following the localization task varied from day to day, and progressed from simple to complex (Figure 4.04 for overview and Appendix B for detailed day-by-day tasks). Participants performed both localization and recognition tasks, and transitioned from non-cluttered environments (black felt board) to more cluttered environments (black felt wall: Debris, such as a desk, doorway, and various equipment, was present on the left and right as participants approached the wall. Participants were warned when they focused on debris that the target object was not in view). Training was dynamically adapted to fit the participants learning rate and vOICe interpretation weaknesses. Additional time was spent on tasks of particular difficulty to each participant.

Training attempted to integrate and utilize as many modalities as possible. In the last session of training each day, sighted participants performed on the computer a left-right circle localization task, which asked the participants if a circle is on the left or right in an image or on the left or right in a vOICe sound of that image. The task first displayed just images for the localization task, then played vOICe sounds at the same time as images presented, and finally just played the vOICe sounds. Although this computer task was relatively simple (just indicating if a circle is on the left or right with vision and/or vOICe), it allows for the integration of information across modalities, which may aid in the development of crossmodal plasticity. (Note: blind participants could not perform this task due to the visual element of the task.)

fMRI Tasks

Overview

Six separate tasks were performed by sighted subjects in each fMRI scanning session. The 4 relevant tasks to Chapter 4 will be described here; the remaining 2 tasks will be detailed in Chapter 5. The blind participants performed 4 separate tasks, 3 of which will be describe in Chapter 4, and 1 of which will be described in Chapter 5.

vOICe Noise Pause Detection

The first task was detection of a pause within a vOICe sound encoding an image of white noise (Figure 4.05). During this task participants fixated on a cross, and listened to a vOICe sound played twice (2 second duration). The vOICe sound's pause was either at the beginning, middle, or end. If the sound had a pause, the participant pressed 1; if there was no pause, the participant responded by pressing 2 (24 percent of trials had no pause, while 76 percent of trials had a pause). The participant performed 50 trials of the pause detection task, and was not told that the noise sound was from the vOICe. This task will be referred to as the vOICe noise or vOICe noise pause detection task in the rest of this chapter.

The vOICe noise was encoded with the vOICe software from a set of 10 white noise images generated in MATLAB. The function "random" in MATLAB was used to generate random numbers in a uniform distribution between 0 and 256 for each element, and then each element value was rounded to the nearest integer. Each element was used to make a matrix of 650 x 795 elements (or pixels). The matrices were converted to grayscale and saved as bmp files. The bmp files were loaded into a .mat file (which was used in the experiment) as truncated images of a 600 x 795 size in order to match the size of the localization images (localization task is detailed in Chapter 5).

Vision Noise Pause Detection

The second task was pause detection of a white noise visual image presentation (same images used in vOICe noise pause detection task) (Figure 4.06). The pause in the image presentation lasted for 0.19 seconds of 2-second continuous image presentation. The participants pressed 1 for pause, and 2 for no pause; 24 percent of trials had no pause, while 76 percent of trials have image pause. The pause could be present at the very beginning, middle beginning or the middle of the image presentation. This task will be referred to as the vision noise or vision noise pause detection task in the rest of this chapter. Note: the main difference between the vOICe noise pause detection and vision noise pause detection is that one task is auditory (vOICe noise pause detection), and the other task is visual (vision noise pause detection).

vOICe Noise Distraction Task

The third relevant task was a distraction task with vOICe sounds (Figure 4.07). Participants were shown a number between or equal to 100 and 149, and were told to count backward from the number in 7s. While participants were counting, a vOICe sound encoding a white noise image was played. Participants were instructed to ignore such a sound if it did play (thus, no task with the vOICe sounds). Participants were not asked to press buttons during this task. Participants performed 50 trials of the counting distraction task before and after vOICe training. This task will be referred to as the vOICe noise distract or vOICe distract counting task in the rest of this chapter.

Pause Detection with Familiar Sounds

The fourth relevant task was detection of a pause within familiar sounds (same experiment layout as Figure 4.05, but with familiar sounds). Two familiar sounds were used: A sound of a beach (2.04 second duration), and a sound from Star Trek (1.27 second duration). The aim of this task was to determine whether vOICe training affected the neural processing of unrelated familiar sounds. During this task, participants were asked to fixate on a cross in the center of their field of view. Participants were asked to respond by pressing 1 if there was a pause in the sound played, and pressing 2 if there was no pause in the sound. The pause could be present at the beginning, middle, or end of the sound, and the sound was the same duration with and without the pause. The participants performed 50 trials of pause detection for each sound before and after vOICe training. These tasks will be referred to as the Beach noise pause detection, Star Trek sound pause detection, or familiar sounds pause detection task in the rest of this chapter.

Blind Participant Tasks

Blind participants performed the vOICe pause detection, the vOICe noise distraction and the pause detection with familiar sounds tasks. They performed the same three tasks as the sighted participants, except for the way instructions were given, but for the sake of convenience, we count them as different tasks (altogether, 7 tasks for Chapter

4 and 3 tasks for Chapter 5). Instructions for the tasks were read aloud by the Macintosh Computer Speech utility and recorded by QuickTime into an audio mov file. These mov files were converted into wav files, and loaded into MATLAB to be played at the beginning of the experiment. The counting starting numbers for the vOICe distraction task were recorded, saved, and loaded into MATLAB in the same manner, and then programmed to automatically be read aloud at the beginning of each trial. All other elements of the experimental design were the same for the blind participants, including the vOICe training.

fMRI Data Acquisition

A Siemens TIM-Trio 3 Tesla MR scanner in the Caltech Brain Imaging Center (CBIC) was used to collect the neural imaging data. A 12-channel phased-array headcoil and MR Confon headphones were used for data collection and audio delivery, respectively. The imaging parameters were: TR = 2.25 seconds, 38 slices in ascending order, and [3,3,3] millimeter voxel size. Participant responses were recorded with a four-button response box within the scanner, of which two buttons were used. Images were presented with a projector image reflected off of a mirror attached to the headcoil and into the participants view. Eye positioning information was recorded for select tasks using a Restek eye-tracking camera attached to the headcoil, and recorded on a lab computer using PowerDirector software. T1 structural scans were acquired in addition to fMRI functional scans for each participant in either the first or second fMRI scanning session, and were coregistered with functional data. The T1 imaging parameters were: TR = 1.5 seconds, and [1,1,1] millimeter voxel size.

vOICe Experiment Layout

Week 1	Sunday	Monday	Tuesday	Wednesday	Thursday	Friday Pre-training fMRI scan 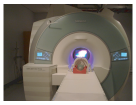	Saturday
Week 2	Sunday	Monday vOICe Training (1 hour) 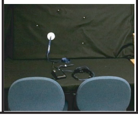	Tuesday vOICe Training (1 hour) 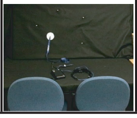	Wednesday vOICe Training (1 hour) 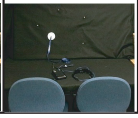	Thursday vOICe Training (1.5 hour) 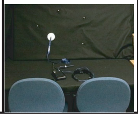	Friday vOICe Train. (30 min) 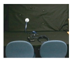 Post-training fMRI scan 	Saturday

Figure 4.02. vOICe experiment layout. Schematic diagram showing a typical schedule of the fMRI and vOICe training design. A fMRI scan preceded and followed a training period of four days and about five hours. The fMRI scanning sessions both contained the same tasks, and the vOICe training changed in each session.

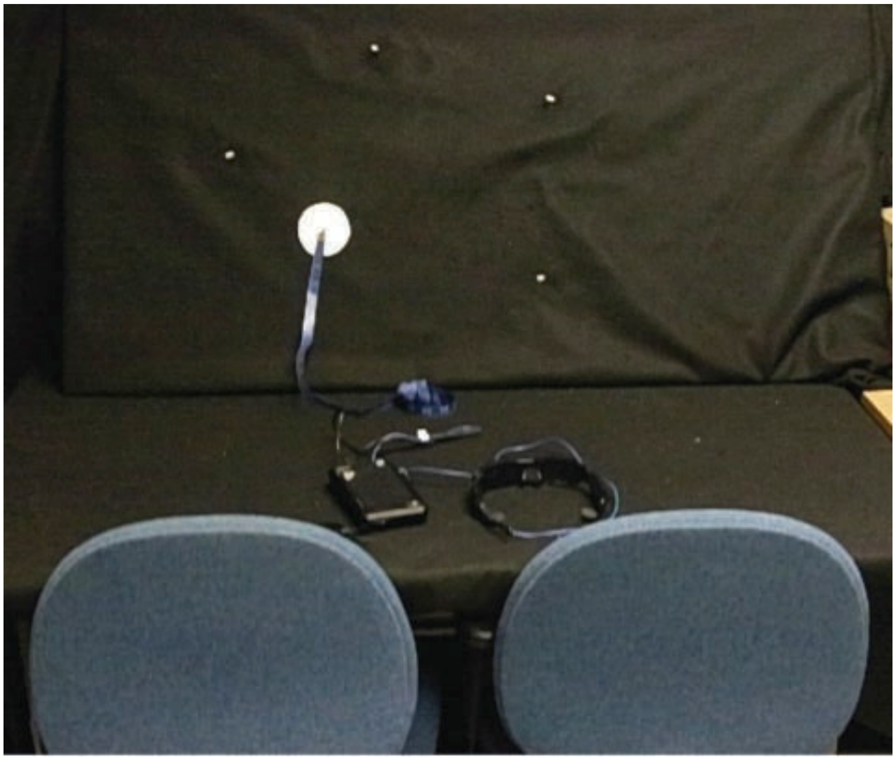

Figure 4.03. vOICe localization task setup. Participants performed a localization task to assess their progress on each day of vOICe training. This image depicts the localization task setup, with the vOICe glasses and computer on the table, and the white dot that participants located and reached for on the black-felt-covered wall. The white markers indicate the other four locations at which the white dot can be placed (the markers are not present during the experiment, but rather replaced with nearly invisible black velcro).

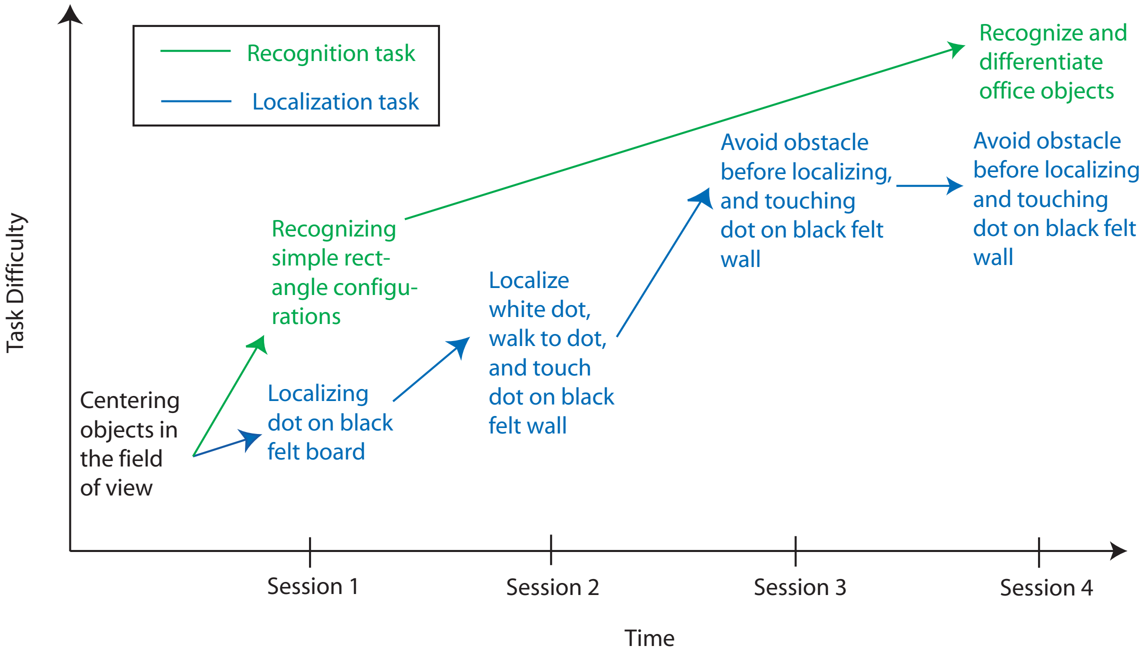

Figure 4.04. vOICe training flow chart. Training was performed on the sensory subsitution device (the vOICe) between the pre-training fMRI scan and post-training fMRI scan. This diagram outlines the tasks performed in training and a general time progression of those tasks as a function of difficulty. The localization and recognition tasks are separated into blue and green colors. Each training session was about an hour in duration, but varied to some degree based on each participant's speed at completing each training task.

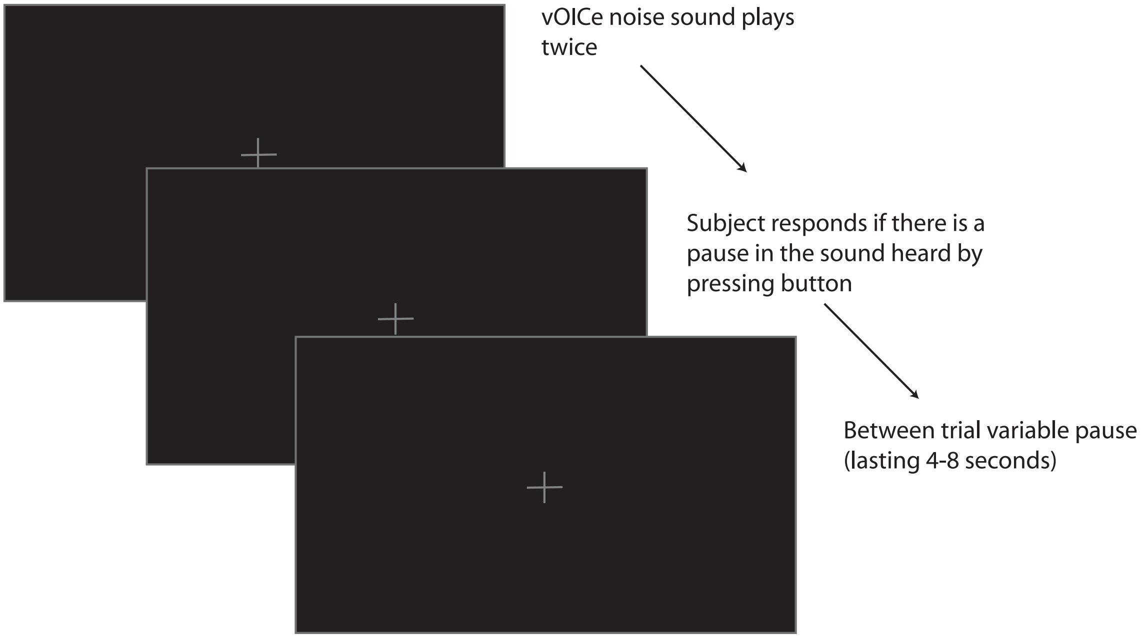

Figure 4.05. fMRI experiment diagram of the auditory pause detection task. Experiment layout of the vOICe noise pause detection task. The pause can be present at the beginning, middle, or end of the vOICe sound. The vOICe sound with the pause is played twice to lengthen the stimulus duration to 2 seconds. The familiar sound pause detection task is designed be the same format as vOICe noise pause detection task. The auditory pause detection task (vOICe noise and the familiar sound pause detection) was performed in both scan sessions.

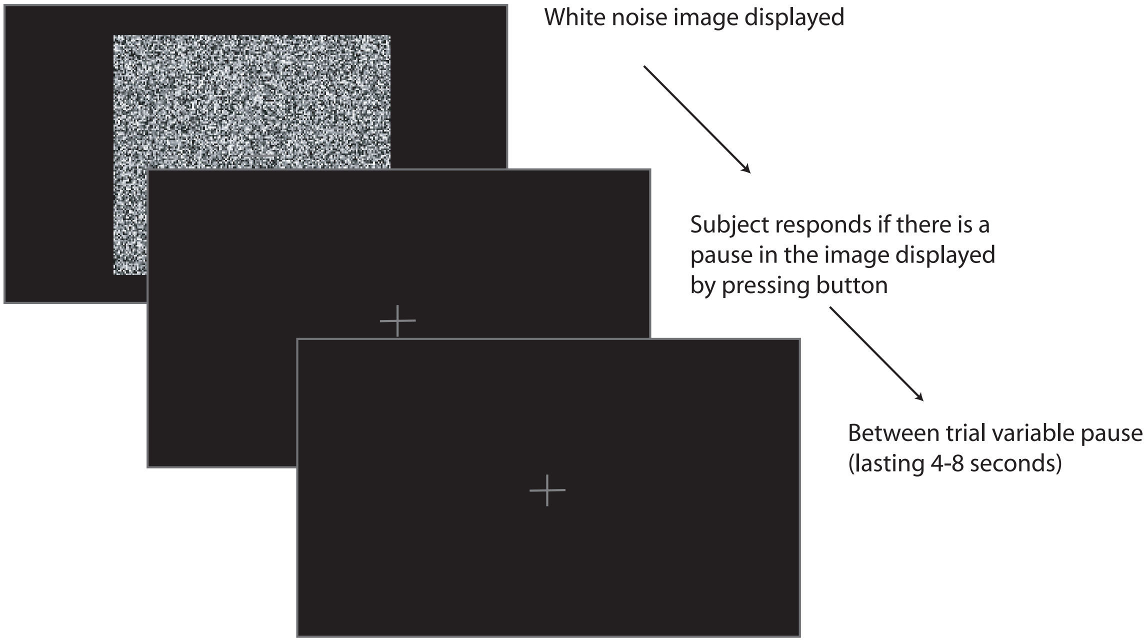

Figure 4.06. fMRI experiment diagram of visual pause detection task. The visual pause detection task used white noise images and asked participants to determine whether the image paused during its presentation. The visual pause detection was used as a control for the vOICe pause detection experiment. The visual pause detection task was performed in both scan sessions.

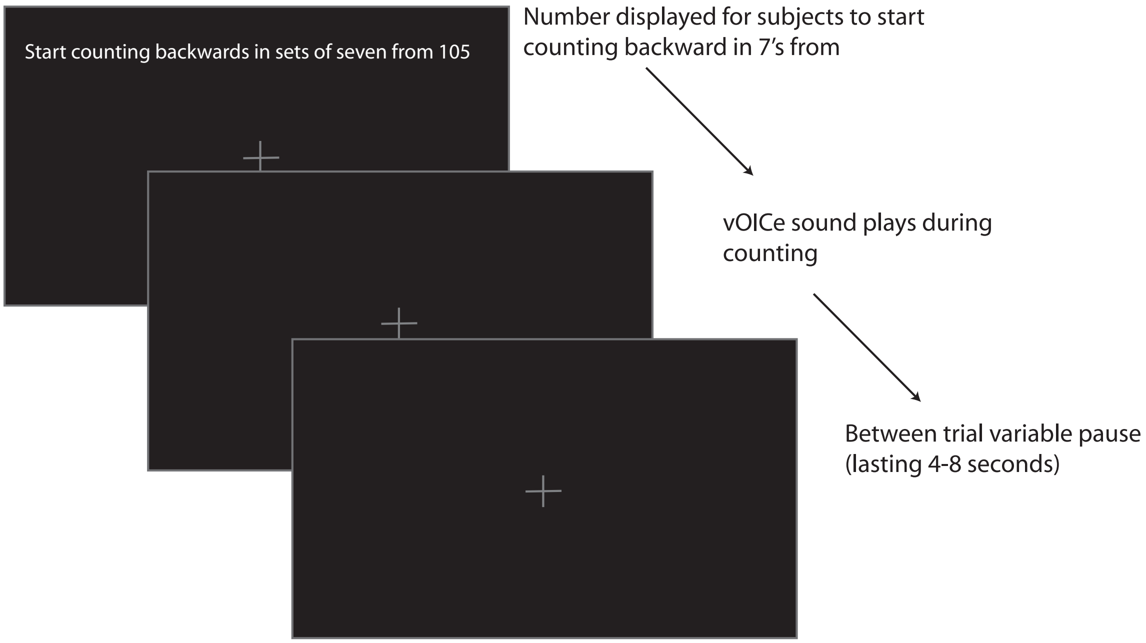

Figure 4.07. fMRI experiment diagram of the vOICe distract counting task. The vOICe distraction counting task presented a number between 100 and 149, and required participants to count backwards in 7s. While participants were counting, a vOICe sound encoding a white noise image was played. Participants were told to ignore the sound played. The vOICe distraction counting task was performed in both scan sessions.

fMRI Data Preprocessing

fMRI preprocessing of the imaging data was performed in SPM8 (The Wellcome Trust Center for Neuroimaging, at the Institute of Neurology at University College London (UCL), UK) (Ashburner et al., 2011). Functional scans were corrected for slice time acquisition, and movement (via image realignment). The co-registration of participant functional and structural images was performed along with normalization to the standard space defined by the ICBM, NIH P-20 project (Ashburner, et al., 2011) and smoothing by an Gaussian kernel of 8 mm full-width at half maximum (FWHM).

fMRI Data Postprocessing (Statistical Analysis)

One general linear model (GLM) was generated, including all 6 fMRI tasks and both the pre-scanning and post-scanning sessions for each participant. High pass filtering was performed in the model specification stage of processing (128 second filter width). No within-participant regressors were used except for standard movement regressors and 12 session constants (one constant per task, 6 tasks pre-training and 6 tasks post-training for sighted participants). The GLM was estimated with a classical algorithm (Restricted Maximum Likelihood). Forty-three contrasts were generated for each sighted participant in order to explore both differences between pre- and post-training conditions, as well as within session comparisons such as localization of a dot on the left *vs.* the right. The resulting contrasts were summed in a level 2 processing, across all 10 sighted participants. Blind participants were processed individually with a total of 10 contrasts for four tasks in each scan session.

fMRI Data Covariate Analysis

Covariate analyses were used to determine whether any neural activation correlated with a behavioral measurement. A second-level analysis in SPM8 was used in which the contrasts from each participant were summed and a covariate numeric value was entered for each participant in a corresponding matrix. The resulting neural activation from the analysis correlated in strength with the numeric magnitude of the covariate values entered. Covariate values were determined by either the experiment questionnaire (Appendix C) or localization task performance data.

fMRI Data Visualization

Data visualization for both Chapter 4 and Chapter 5 was performed in SPM8. For the section view of Figures 4.12, 4.13, 4.15, 5.5, and 5.7, the neural activation (BOLD functional imaging data) was overlaid on the SPM8 canonical individual T1 structural image. Inflated brain images of Figures 4.12, 4.13, 4.15, 5.5, 5.7, and 5.9 were generated using the render function in SPM8 with the canonical cortical surface image.

Behavioral Data Statistics

ANOCOVA and correlation analyses were performed in MATLAB using the aoctool, and corr functions.

Results

Behavioral Results

Localization was measured daily during vOICe training at the beginning of each training session (the details of the localization evaluation are in the method section under vOICe training procedure). The inaccuracy of participants’ reach for a white circle on a black felt board with vOICe, normal vision, and random reaching (*i.e.,* no vision or vOICe) is plotted in Figure 4.08 for all of the sighted participants ($N = 10$), and Figure 4.11 for all of the blind participants ($N = 4$). The inaccuracy of the sighted participants' reach decreased with training time (or training sessions, about 1 hour per session) at a rate greater than the random reaching. The slope of the random reaching (*i.e.,* no vOICe or visual input) for the sighted participants is not significantly different from the slope of their vOICe reaching; however, the intercepts are significantly different between random reaching and vOICe reaching (ANOCOVA analysis, $p_{slope} < 0.39$, $p_{Intercept} = 0$). In other words, the sighted participants performed significantly better than random reaching with vOICe at the beginning of training (represented by intercept). However, their learning improvement (represented by slope), while improving at a rate greater than random reaching, was not significantly better. In part, this result is due to the intuitive nature of the localization task; therefore, the task can be learned well in the first half of the first training session trials, generating a large difference between vOICe performance and random reaching. However, as training progresses, participants learn the environment and the most likely spatial regions for the dot location, allowing for improvement at the random reaching control task. This control improvement is then compared to the vOICe task improvement, making it more difficult for the vOICe improvement to be significantly larger. Further, a similar task in the literature by Auvray *et al.* in 2007 showed that reaching for a 4 cm. ball using the vOICe device on a table did not significantly improve in accuracy over two 1-hour training sessions.

Localization improvement with training indicates increased hand-camera (*i.e.*, hand-head) coordination, spatial perception with vOICe, and centering technique (as described below). When participants begin using the vOICe device (Figure 1.4), they must integrate cognitive information (such as the vOICe encoding principles, and camera location) with perceptual experience and motor commands. Critical elements of that learning process are learning search strategy (the field of view is more limited with vOICe than natural vision), the limits of the camera field of view, the camera position relative to their hand and body, and the sound of different spatial positions such as the top of the field of view, and center of the field of view. The relation between the spatial position of the target in the field of view of vOICe and the field of view in real space can then be used to modulate and guide hand movement during localization.

A training technique of centering then reaching often aids participants in learning vOICe localization. The participant is taught to first locate the object and then center the object in the field of view, therefore identifying the objects position in vOICe coordinates. The participant then tactilely locates the camera on the glasses with their reaching-hand, identifying the direction of their gaze and the physical real-world coordinates of the vOICe field of view. Finally, the participant reaches in the direction that the camera is pointed. This method helps participants improve their accuracy, because it forces participants to consciously note the direction of the camera. Without this conscious reminder of camera direction, participants can easily forget that their head is slightly tilted, altering the location of the center of the field of view in real space. Further, the centering of the sound then camera position identification joins the virtual vOICe space with the real space that the camera’s field of view covers, enabling better integration of two types of information.

Learning the spatial limits of target placement is especially relevant to searching strategy as well as improvement at random reaching. Often, at the beginning of training, participants will not explore the full extent of the black felt board where the target is located; rather, they will explore only the upper or lower half, or left or right half of the board. When they begin to become confused or frustrated at not locating the target within their limited search radius, the experimenter often provides a hint of the un-searched section of board. As the participant progresses in the task, they learn where the target can and cannot be located, reducing confusion in their search strategy. This learning of the limits of the potential target locations is likely the reason that random reaching improves slightly with training time, as participants will likely direct even their random reaching to the general area of target locations. By reducing search time in unnecessary spatial locations, learning the target space is also important to improving participants' task efficiency.

Sighted participant localization task performance also seems to show a ceiling effect. The sighted participant individual localization performance *vs.* training session is plotted in Figure 4.09. While participants have a wide range of starting localization accuracy in session 1, their final localization performance range has narrowed to a much smaller range. Another way of representing this effect is in Figure 4.10, where the slope and intercept for each participant are plotted on a scatter plot (each data point is a different participant). Interestingly, the slope and intercept across participants are significantly negatively correlated ($rho = -0.7464$, $p < 0.01$). This means that when the starting position (*i.e.,* intercept), increases (*i.e.,* becomes more positive, more inaccurate) the slope decreases (*i.e.,* becomes more negative, or higher learning rate). Therefore, independent of where participants begin their performance of the localization task, the learning rate compensates to make their end performance within a small range of localization accuracy. This effect may be due to a limiting factor that prevents the early-high-performance participants from improving the same amount as the early-low-performance participants. It may be true that the participants performing better at the beginning of training better translate their cognitive knowledge to spatial interpretation and hand-camera coordination in contrast to those that perform worse at the beginning of training. However, as training continues, both the early and late learners are limited by the resolution of vOICe vertically and horizontally, hand-camera coordination, and the lack of visual feedback during the reaching movement. It is useful to note, though, that this “ceiling” could still possibly be overcome by longer, more intensive training than used in this experiment.

Low-vision and blind participants were also trained on the vOICe device, and performed the localization task (Figure 4.11). Panel A of Figure 4.11 shows the localization results for a severe low-vision participant, FZ (visual acuity: 20/420), with late-onset visual impairment. His performance indicates a rapid rate of learning (FZ slope: −1.36, the more negative the better), much greater than the sighted participants (sighted participant slope: −0.63); however, his initial performance is also much worse (FZ intercept: 11.22 inches, sighted participant intercept: 7.38 inches). His results thus follow a qualitatively similar trend of the "ceiling effect" to that in the sighted. The blind participants ($N = 3$) (participant details in methods) performed similarly to the sighted on the improvement of localization with vOICe (blind vOICe slope: −0.41), but had a larger slope for the control random reaching than the sighted (blind control slope: −0.55; sighted control slope: −0.23). It is unclear exactly why the blind participants random reaching improved so much; it may be an artifact of the limited number of trials (only 10 trials per day). It is also possible that training on the vOICe device improved the blind participants' deficit in spatial awareness. This improved spatial awareness could have been measured as an improved sense of the target space that they unconsciously reached toward during random reaching. The final possibility is that because the blind have a heightened sense of hearing, they may (toward the end of training) have been able to barely hear the general direction of the dot placement.

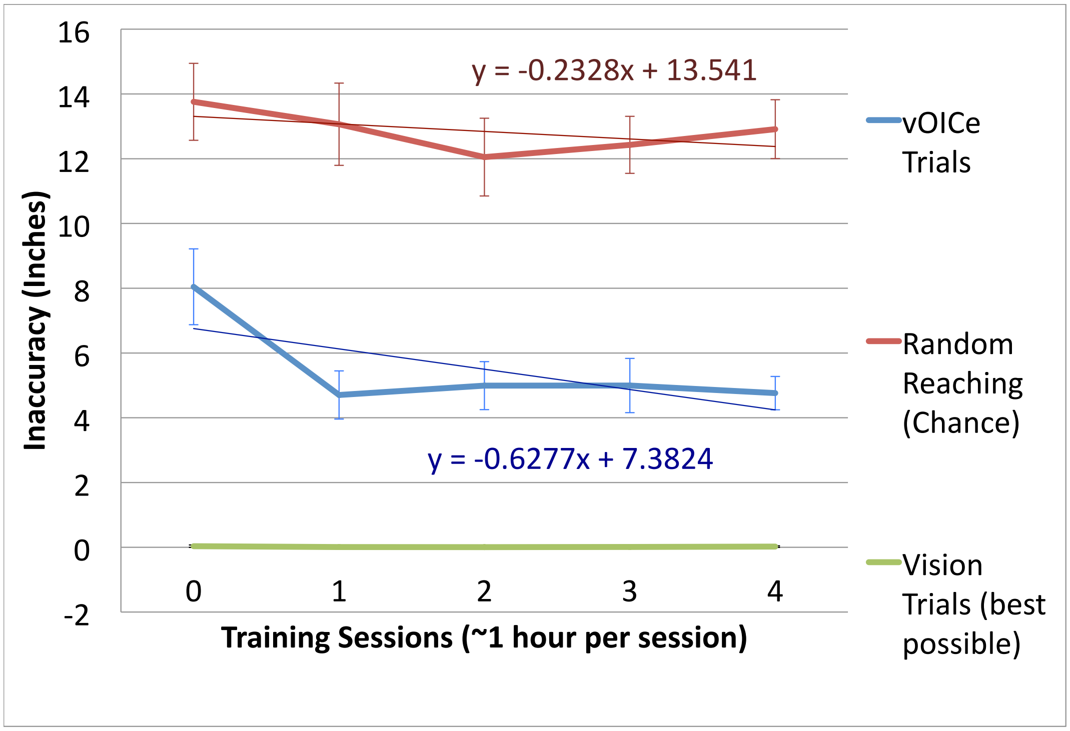

Figure 4.08. Sighted participant localization behavioral performance. Sighted fMRI participants ($N = 10$) performed a localization task in each training session (Figure 4.03), where they reached for a white dot on a black felt board. The spatial inaccuracy of their reach was recorded in inches. This inaccuracy is plotted when using vOICe to localize the dot, when using vision to localize the dot, and when using neither vOICe or vision (*i.e.,* random reaching).

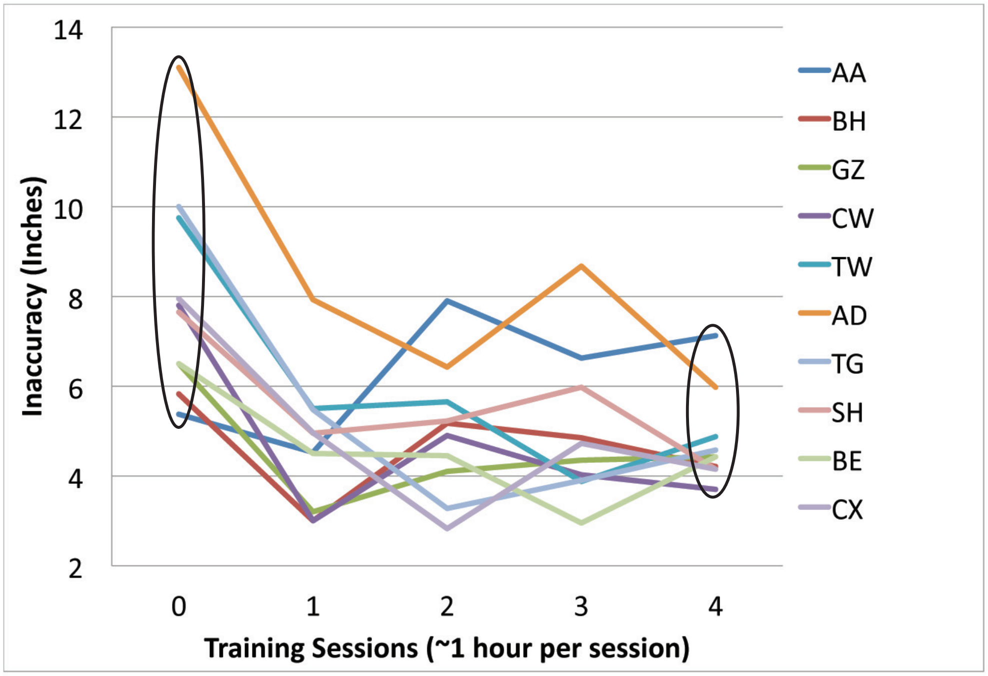

Figure 4.09. vOICe localization behavioral performance in individual participants. Sighted fMRI participants (*N* = 10) performed a localization task in each training session (Figure 4.03), where they reached for a white dot on black felt. The spatial inaccuracy of their reach was recorded in inches. This inaccuracy is plotted when using vOICe to localize the dot, when using vision to localize the dot, and when using neither vOICe or vision (*i.e.,* random reaching) in Figure 4.08. This plot shows the individual participants' performance at the vOICe device alone. This plot shows that the range of initial localization inaccuracies (elipse on left) is much wider than the range of final inaccuracies (elipse on right). The narrowing in performance range with training sessions supports the ceiling-effect hypothesis in Figure 4.10.

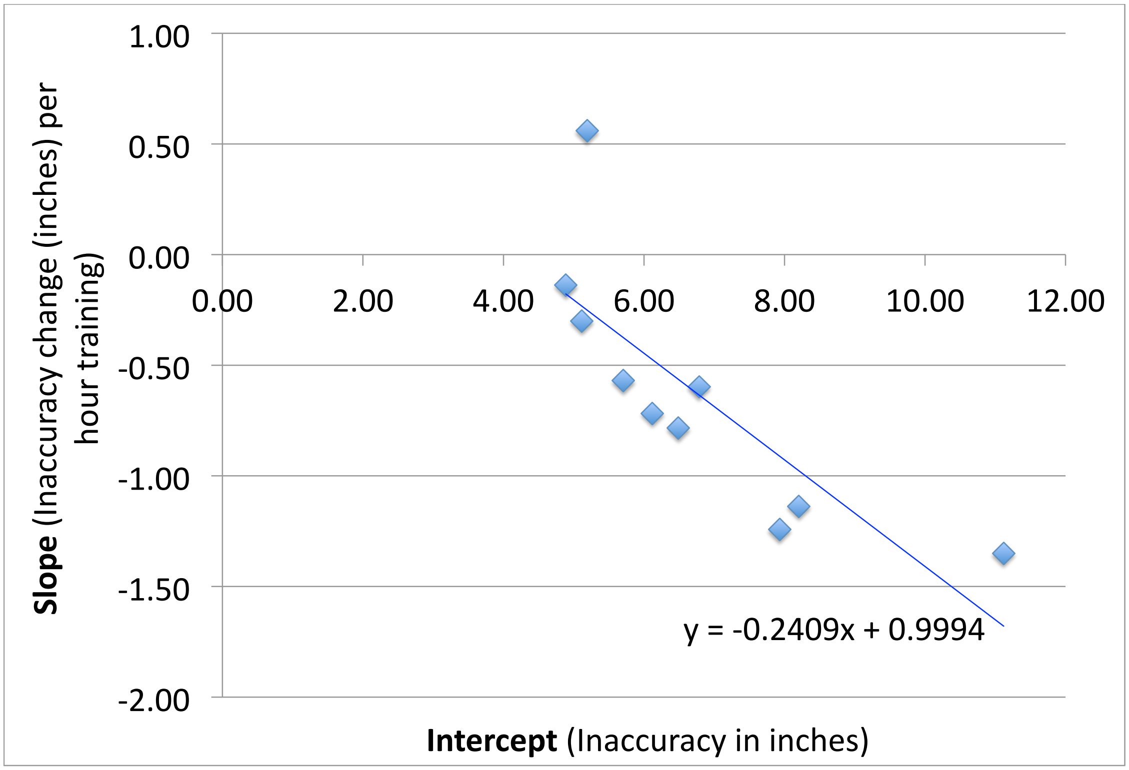

Figure 4.10. Sighted localization behavioral performance, slope *vs.* intercept. fMRI participants performed ($N = 10$) a localization task in each training session (Figure 4.03), where they reached for a white dot on black felt. The spatial inaccuracy of their reach was recorded in inches. The slope and intercept of this vOICe localization inaccuracy *vs.* training session plot for the individual participants is plotted above (each data point is a different participant) ($rho = -0.7464$, $p < 0.01$). The correlation between the slope and intercept of participants' localization performance indicates a possible ceiling effect, where the performance of participants with initially low inaccuracy improved at a slower rate (less negative slope) than participants with initially high inaccuracy. In effect, all participants asymptoted to a similar final performance, independent of their initial inaccuracy with vOICe localization. This indicates that specific elements of this vOICe training or the vOICe in general are limiting further improvement. These limitations

could possibly be overcome with more extensive training.

A

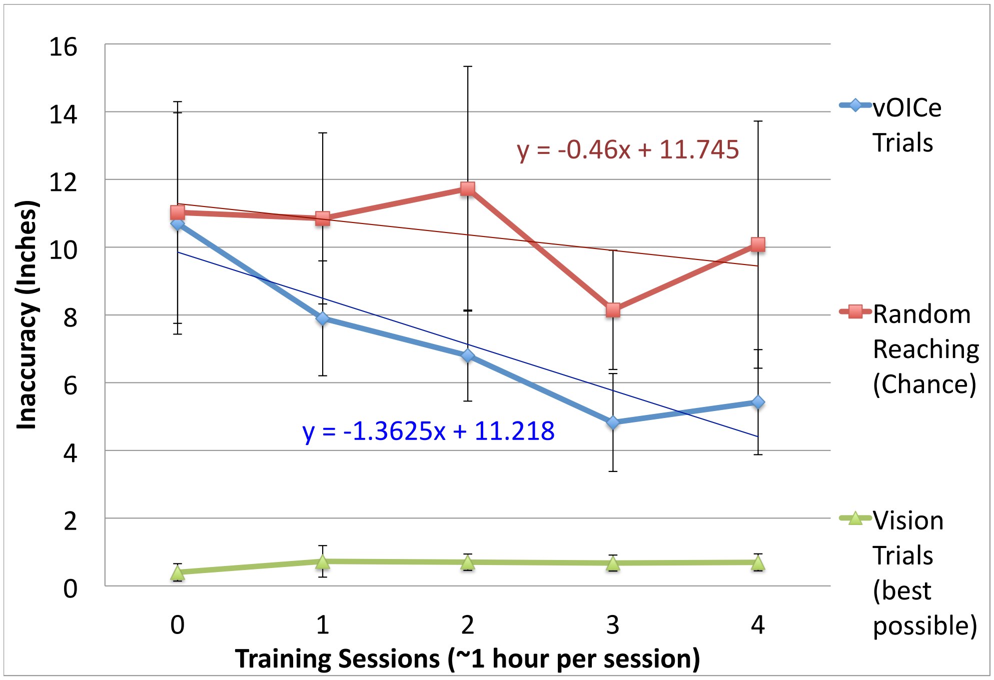
16
14
12
10
8
6
4
2
0
Inaccuracy (Inches)
0
1
2
3
4
Training Sessions (~1 hour per session)
y = -0.46x + 11.745
y = -1.3625x + 11.218
vOICe Trials
Random Reaching (Chance)
Vision Trials (best possible)

B

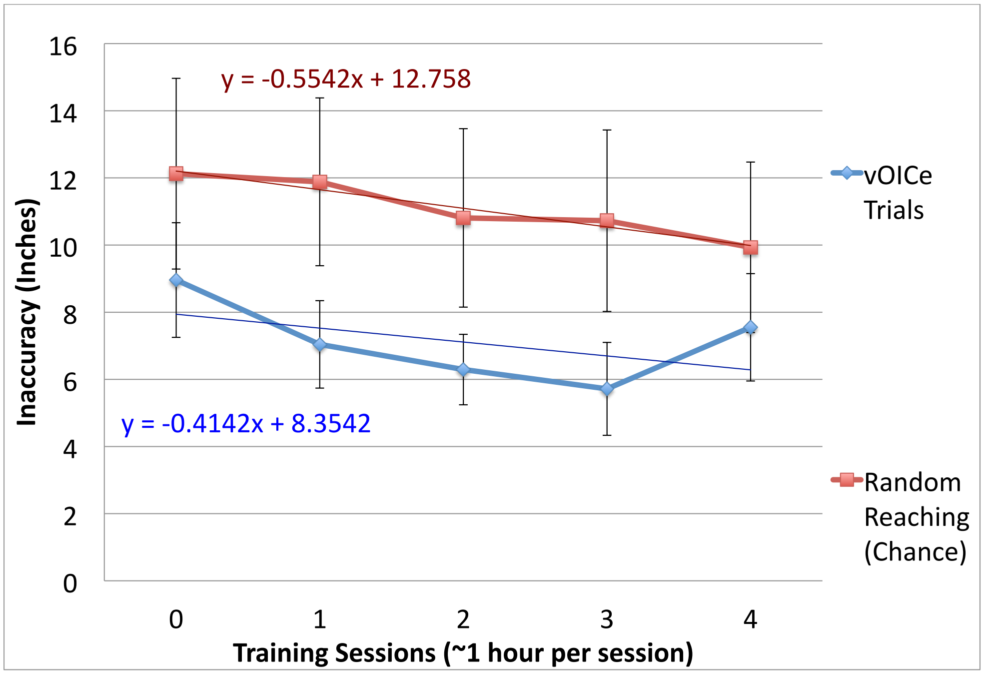
16
14
12
10
8
6
4
2
0
Inaccuracy (Inches)
0
1
2
3
4
Training Sessions (~1 hour per session)
y = -0.5542x + 12.758
y = -0.4142x + 8.3542
vOICe Trials
Random Reaching (Chance)

Figure 4.11. Blind and severe low-vision participant localization behavioral performance. Panel A shows a severe low-vision fMRI participant (*N* = 1) localization task performance. Panel B shows blind fMRI participants (*N* = 3; one late blind and two congentially blind) localization task performance. In each session (Figure 4.03), participants reached for a white dot on black felt. The spatial inaccuracy of their reach was recorded in inches. This inaccuracy is plotted when using vOICe to localize the dot, when using neither vOICe or vision (*i.e.,* blind trials or random reaching), and when using vision alone (only with the low-vision participant).

fMRI Imaging Results

Sighted Participant Imaging Results

Two fMRI tasks are the primary focus of testing the automaticity of crossmodal plasticity with vOICe: The vOICe-noise pause-detection task, and the vOICe-noise distraction task (see the methods for the task details). The contrast of vOICe noise pause detection [Post-training – Pre-training] was used to test whether training on vOICe induced crossmodal plasticity with visual activation (Note: [Post-training – Pre-training], and [Post – Pre] will both be used to indicate that the pre-vOICe-training scans were subtracted from the post-vOICe-training scans). Figure 4.12 and Table 4.1 show the results for this contrast on 10 sighted participants. Sighted participants were found to have significant activation in Brodmann Area (BA) 39 for this task. A small volume correction for BA 39 yielded pvalues less than 0.05, when a sphere of 10 millimeter radius (mm) was used (Table 4.1).

The contrast of vOICe noise distraction task [Post-training – Pre-training] was used to investigate the impact of vOICe training on automatic crossmodal visual activation in 10 sighted participants. Figure 4.13 and Table 4.2 show the results for this contrast. Significant activation was found in Brodmann Areas (BA) 41, 19, and 18 among others. A small volume correction for BA 19 and 18 yielded pvalues not less than 0.05, when a sphere of 10 mm radius was used (Table 4.2). Nonetheless, a small volume correction with 5 mm radius sphere does yield pvalues less than 0.05 (BA 19 [−39 −76 −2] $p < 0.02$, BA 19 [−33 −67 −2], $p < 0.04$, BA 18 [−24 −79 19] $p < 0.03$). Therefore, the small variation in the strigency of the multiple comparisons correction makes the activity significant, which may indicate relatively smaller cortical volumetric changes as the neural correlates of the training effect.

The neural activation results for the pause detection task with familiar sounds are presented in Table 4.3. The contrast of familiar sounds pause detection [Post-training – Pre-training] was used to identify changes in neural processing engendered by the training on the vOICe device. For this Post-Pre contrast, BA 39 and 40 were activated similarly to the vOICe noise pause detection task Post-Pre contrast, but no early visual areas were activated.

In both the vOICe-noise pause detection and the familiar-sound pause-detection tasks, BA 39 was significantly activated in a post-training minus pre-training contrast. BA 39, as a part of the angular gyrus, is known for many different types of functions ranging from language processing, calculation, and visual spatial processing (Bernal & Perdomo; Delazer et al., 2003; Inui et al., 1998; Kohler, Kapur, Moscovitch, Winocur, & Houle, 1995). While the visual spatial processing is most relevant to the task in this experiment, the other functions can not be entirely ruled out, though improbable (the participant was not reading or calculating). In crossmodal interactions and sensory substitution fMRI studies, BA 39 is also a frequent participant. As mentioned earlier, when the angular gyrus is damaged, participants lose the bouba-kiki effect, a common and strong shape-to-sound crossmodal mapping (Ramachandran & Hubbard, 2003). In sensory substitution studies, BA 39 is frequently activated during SS interpretation tasks (Plaza, et al., 2012; Poirier, De Volder, Tranduy, et al., 2007). Therefore, it is likely that BA 39 is mediating the crossmodal integration that is essential to the spatial and visual interpretation of vOICe sounds.

The vOICe distraction task (counting backwards) activated BA 19 and 18 when the pre-training scans were subtracted from the post-training scans. This visual activation in early visual areas (V3 and V2) could be generated by visual imaginings of numbers and shapes. While the post- and pre-scanning session subtraction should remove this visual imagining (there is no reason the visual imagining should not occur in both sessions and therefore cancel out), it is also possible that vOICe training strengthened visualization, making it easier after training. An experiment questionaire and visualization covariate will further answer these questions in the following pages.

If the visual activation in the vOICe distraction task [Post – Pre] is due to the vOICe training, then the visual activation shows that crossmodal plasticity can be activated automatically (*i.e.,* with attentional distraction). As highlighted in the introduction to the chapter, this is an entirely new result to the sensory substitution field, and indicates that sensory substitution processing might not be entirely processed in a cognitive top-down fashion. It shows that the crossmodal plasticity is resistant to attentional load and therefore at the neural level acts more like vision than was ever suspected. This result may be the critical first step in generating SS training procedures and encoding algorithms that capitalize on this automatic crossmodal processing to obtain stronger, more intuitive SS interpretation and use.

A

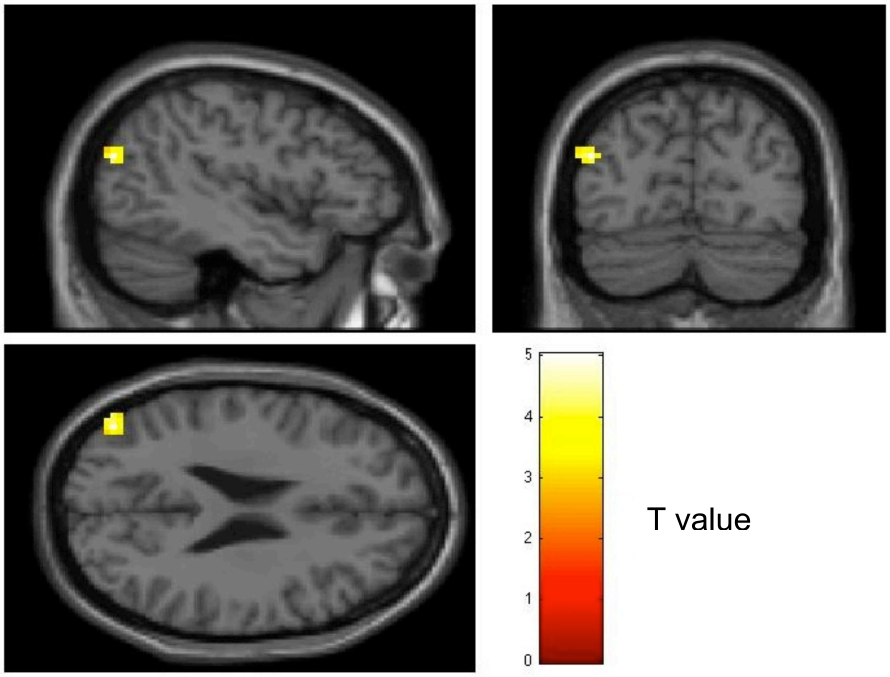

B

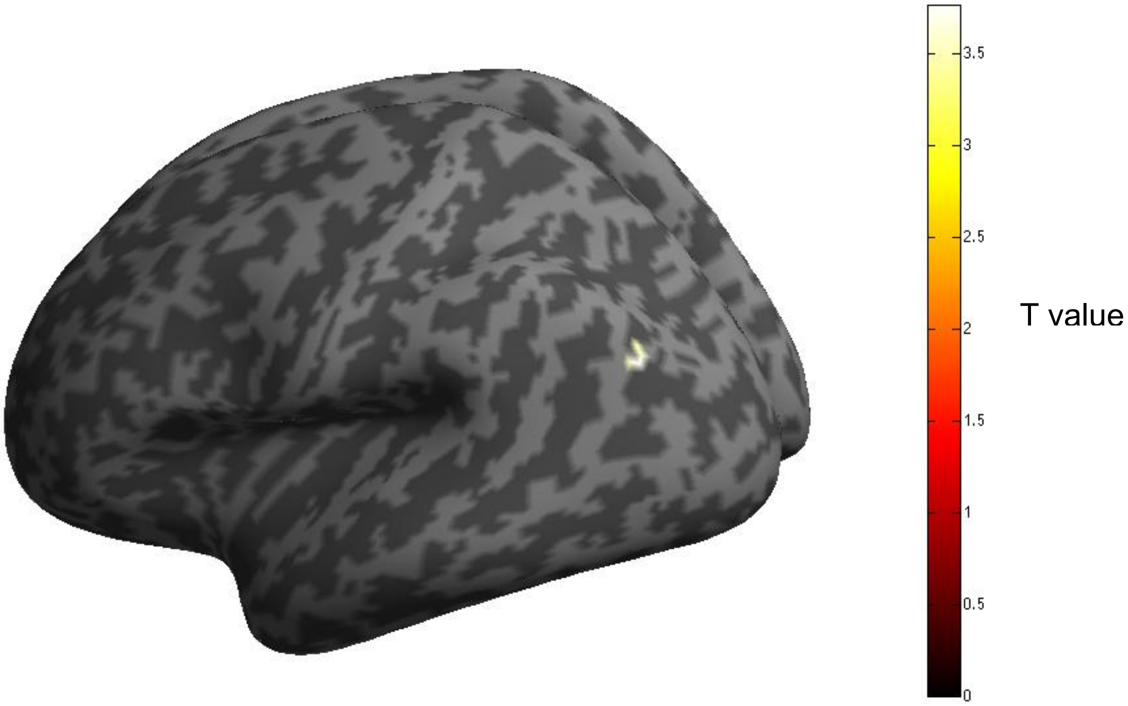

Figure 4.12. fMRI data: Post – pre training vOICe noise sighted participants. The neural imaging result is displayed for post-vOICe-training in contrast to pre-vOICe-training for the vOICe noise pause detection task in sighted participants ($N = 10$). Imaging data presented shows activation in BA 39, and is $p < 0.009$ uncorrected and clusters of 10 voxels or more. Further correction for multiple comparisons is shown in Table 4.1. The detailed description of methods for fMRI data display are in the Chapter 4 methods.

Sighted Participants ($N = 10$)						
Region	BA	Side	x	y	z	p_{uncorr}
vOICe Noise Pause Detection [Post – Pre]						
Middle Temporal Gyrus	39	L	−45	−76	25	0.000
- small volume-corrected peak						0.029*

Table 4.1. fMRI data: Post – pre training vOICe noise pause detection sighted participants. Imaging results for sighted participants when comparing post-vOICe-training scan and the pre-vOICe-training scan ($N = 10$). All regions were limited to $p < 0.009$ uncorrected and 10 voxel cluster threshold (p_{uncorr} refers to the peak level p_{uncorr}). The small volume correction was for a sphere of 10 millimeter radius around the cluster center, and the pvalue shown (indicated by asterisk, *i.e.*, *) is for the peak level FWE-corrected. Brodmann area localization was performed on the talaraich client for nearest grey matter. Any clusters without nearest grey matter within +/− 5 mm are not included.

A

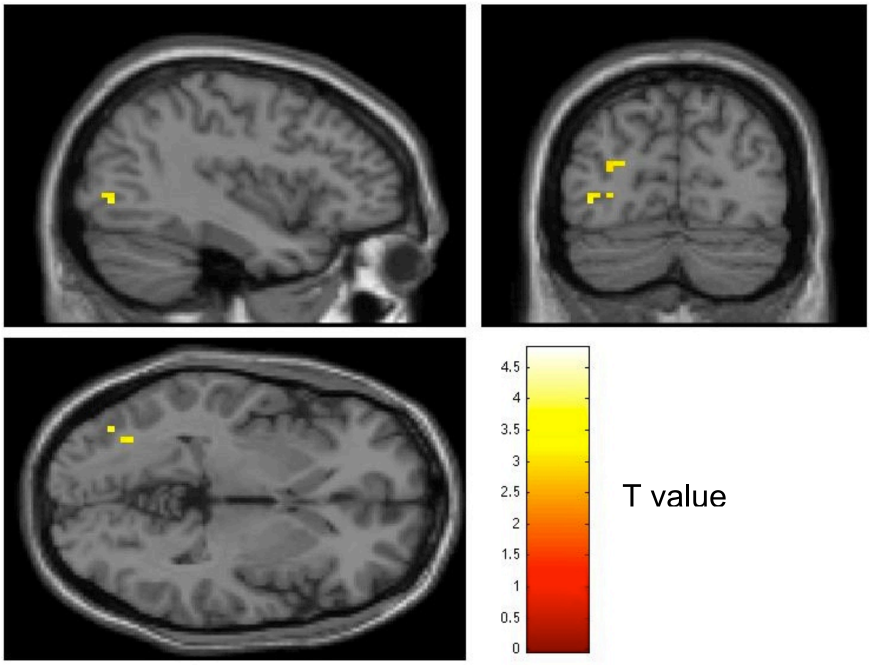

B

Figure 4.13. fMRI data: Post – pre training vOICe-noise distract task in sighted participants. The neural imaging result is displayed for post-vOICe-training in contrast to pre-vOICe-training for the vOICe-noise distract task in sighted participants ($N = 10$). Imaging data presented shows activation in BA 19 and 18 among other regions, and is $p < 0.009$ uncorrected and clusters of 10 voxels or more. Further correction for multiple comparisons is shown in Table 4.2. Methods for fMRI data display are in the Chapter 4 methods.

Sighted Participants ($N = 10$)						
Region	BA	Side	x	y	Z	p_{uncorr}
vOICe Distract Counting [Post – Pre]						
Superior Temporal Gyrus	41	R	39	−31	4	0.000
Inferior Occipital Gyrus	19	L	−39	−76	−2	0.003
- small volume-corrected peak						0.074*
Lingual Gyrus	19	L	−33	−67	−2	0.006
- small volume-corrected peak						0.117*
Cuneus	18	L	−24	−79	19	0.004
- small volume-corrected peak						0.096*
Middle Occipital Gyrus	19	L	−33	−73	19	0.006
Middle Occipital Gyrus	19	L	−33	−79	13	0.008
Posterior Cingulate	29	L	0	−52	10	0.005
Posterior Cingulate	30	L	0	−43	19	0.006

Table 4.2. fMRI data: Post – pre training vOICe noise distract task in sighted participants. Imaging results for sighted participants when comparing post-vOICe-training scan and the pre-vOICe-training scan ($N = 10$). All regions were limited to $p < 0.009$ uncorrected and 10 voxel cluster threshold (p_{uncorr} refers to the peak level p_{uncorr}). The small volume correction was for a sphere of 10 millimeter radius around the cluster center, and the pvalue shown (indicated by asterisk, *i.e.*, *) is for the peak level FWE-corrected. Brodmann Area localization was performed on the talaraich client for nearest grey matter. Any clusters without nearest grey matter within +/− 5 mm are not included.

Sighted Participants ($N = 10$)						
Region	BA	Side	x	y	z	p_{uncorr}
Beach Sound Pause Detection [Post – Pre]						
No Activation						
Star Trek Sound Pause Detection [Post – Pre]						
Insula	13	R	39	−46	19	0.000
Middle Temporal Gyrus	39	R	45	−55	7	0.001
- small volume-corrected peak						0.033*
Thalamus		R	6	−28	10	0.000
Caudate		R	21	−40	10	0.000
Thalamus		L	−6	−34	10	0.000
Middle Frontal Gyrus	6	R	33	−1	64	0.000
Caudate		R	3	5	4	0.000
Caudate		R	3	17	7	0.003
Precuneus	7	R	21	−49	46	0.000
Inferior Parietal Lobule	40	R	33	−43	46	0.001
Inferior Parietal Lobule	40	R	39	−55	46	0.004
Precentral Gyrus	6	L	−24	−16	70	0.001
Precentral Gyrus	6	L	−33	−7	67	0.005
Medial Frontal Gyrus	8	L	−12	38	34	0.001
Postcentral Gyrus	5	L	−24	−43	58	0.001

Table 4.3. fMRI data: Post – pre training familiar sounds sighted participants. Select imaging results for sighted participants when comparing post-vOICe-training scan and the pre-vOICe-training scan ($N = 10$) (only the top 15 clusters of activation are presented in this table; a full list is in Appendix D, Table A). All regions were limited to $p < 0.009$

uncorrected and 10 voxel cluster threshold (p_{uncorr} refers to the peak level p_{uncorr}). The small volume correction was for a sphere of 10 millimeter radius around the cluster center, and the pvalue shown (indicated by asterisk, *i.e.*, *) is for the peak level FWE-corrected. Brodmann Area localization was performed on the talaraich client for nearest grey matter. Any clusters without nearest grey matter within +/– 5 mm are not included.

Visually-Impaired Imaging Results

The visually-impaired participants ranged from severe low vision (participant FZ) ($N = 1$) to total blindness ($N = 3$) (participant details and method alterations to accommodate the blind are in the Methods section). These participant groups were tested for their similarity and differences in crossmodal plasticity and neural processing of vOICe in general. Crossmodal plasticity in the blind is discussed in detail in Chapter 1 (p. 48-49), including visual cortical activation during braille reading. It is also mentioned in Chapter 1 (p. 42) that deactivation of visual cortex with repetitive Transcranial Magnetic Stimulation (rTMS) causes a decrease in sensory substitution performance in the blind, but not in the sighted sensory substitution users. This existing literature indicates that neural plasticity and multimodal integration can be quite different in the blind relative to the sighted, and therefore it is important to compare them directly.

The severe low-vision participant, FZ (visual acuity: 20/420), with late onset visual impairment, performed the fMRI experiment; his neural imaging results are presented in Table 4.4, panel A. In the vOICe noise and familiar sound pause detection, and the vOICe distraction task (post training – pre training) participant FZ had neural activation in Brodmann Area 40. BA 40 is a region previously found to process sensory substitution (SS) and to integrate multisensory information. In sensory substitution processing, BA 40, was found in a study by Ortiz *et al.* to be a significant difference between the blind (with no visual "experience" from SS) and the blindfolded sighted following tactile SS training (Ortiz, et al., 2011). Ortiz *et al.*'s result is similar to our result of BA 40 activation in the fMRI imaging of a nearly blind participant during vOICe tasks. BA 40 was also found to be active in a depth perception study using auditory SS on sighted participants (Renier, Collignon, Poirier, Tranduy, Vanlierde, Bol, Veraart, & De Volder, 2005). BA 40 is “known” as a multisensory region with “super-additive” response to audiovisual speech stimuli (Calvert, Campbell, & Brammer, 2000; James & Stevenson, 2012). Other functions of BA 40 are writing, language comprehension, memory, calculation, motor planning, and music performance (Bernal & Perdomo, 2014). Many of these functions can be ruled out due to the participant, FZ, not reading, listening to language, or performing musically during the tasks in question. Memory of the vOICe training, motor planning, and calculation are possible, but do not apply to all the conditions in which BA 40 was activated (in the distraction task, participants do not press buttons, and are distracted from attentional interpretation of vOICe), whereas multisensory processing does apply to all conditions, making multisensory processes the most probable function of BA 40 in this study.

A late-blind participant, RD, also performed the vOICe fMRI experiment (results in Table 4.4 B; blindness details in methods). Similar to the severe low-vision participant, the late blind participant had activation in BA 40 for all task contrasts, including the vOICe Noise Pause Detection [Post – Pre], the vOICe Distract Counting [Post – Pre], the Beach Sound Pause Detection [Post – Pre], and the Star Trek Sound Pause Detection [Post – Pre]. In addition to this, the late blind participant had activation in BA 39 in the vOICe Noise Pause Detection [Post – Pre], the Beach Sound Pause Detection [Post – Pre], and the Star Trek Sound Pause Detection [Post – Pre]. Brodmann Area 39 is a multimodal region also activated in the sighted participants’ ($N = 10$) imaging results (Table 4.1, Figure 4.12), and is discussed in detail on p. 157. Finally, the late blind participant had neural activation of at least one early visual region, (*i.e.*, BA 17, 18 and 19) in each of contrasts of interest (Table 4.4 B). Therefore, the late blind participant appears to have vigorous crossmodal plasticity that activated early visual regions with vOICe and familiar sound stimuli. This vigorous crossmodal plasticity would be expected in a visually deprived individual, especially one that is late blind. In addition, the late blind participant utilized multisensory regions (such as BA 40) for processing the auditory vOICe input; this would be expected in a late blind participant with normal multimodal integration between vision and audition generated before the onset of blindness.

Two congenitally blind participants performed the vOICe neural imaging experiment (results in Table 4.4 C-D; blindness details in methods). The first, WB, had neural activation in BA 19 for vOICe Distract Counting Task with a [Post – Pre] contrast (Table 4.4 C). Therefore, vOICe auditory stimuli automatically activated visual regions in WB, just like automatic crossmodal activation seen in the late blind participant (Table 4.4 B) and the sighted participants (Table 4.2). Activation in BA 19 has been shown in many sensory substitution imaging studies, as described in Porier *et al.*'s literature review (Poirier, De Volder, & Scheiber, 2007). BA 19 has also been found to be active during braille reading in the blind (Burton et al., 2002). Despite congenitally blind participant WB's visual activation in response to vOICe stimuli (via crossmodal plasticity), he lacked multimodal region activation (such as BA 40 or BA 39) in response to vOICe stimuli. The absence of multimodal region activation may be due to his limited experience with vision and audition interactions. In general, it is likely that a congenitally blind individual has underdeveloped (or absent) multimodal neural processing between these two types (*i.e.* spatial and temporal) of modalities. Therefore, the absence of multimodal region activation in response to vOICe in a congenitally blind participant (when compared to the sighted and late blind participants) is not surprising.

The second congenitally blind participant, SB, had neural activation in BA 18 for the vOICe Noise Pause Detection Task with a [Post – Pre] contrast, and no visual activation for the vOICe Distract Counting Task also with a [Post – Pre] contrast (Table 4.4 D). Therefore, crossmodal plasticity was less likely to be automatic in participant SB. However, in comparison to participant WB (congenitally blind), SB did have multimodal neural activation in BA 40 for several of the constrasts. In a congenitally blind individual, BA 40 may have been taken over by auditory or tactile processing, and therefore indicate a different type of processing than in a sighted or late blind individual.

Overall, two out of three of the blind participants ($N = 3$) had visual activation in the vOICe distract counting [Post – Pre] contrast, indicating automatic processing of vOICe in visual regions. However, in the severe low-vision participant, the vOICe distract counting [Post – Pre] contrast generated BA 40 activation but no early visual activation, meaning that the processing of SS was performed primarily in a multisensory region, rather than in multisensory and visual regions. This difference may be due to the different neural architecture of the low-vision brain (compared to the blind), though it may also be an individual difference. It cannot be conclusive with only one low-vision participant. In general, it can be concluded that the vOICe is processed automatically (*i.e.,* independent of cognitive load) in either multisensory or visual regions for most of the visually-impaired participants tested ($N = 4$).

A

Severe Low-Vision Participant (N = 1) (FZ)						
Region	**BA**	**Side**	x	y	z	p_{uncorr}
vOICe Noise Pause Detection [Post – Pre]						
Inferior Parietal Lobule	40	R	48	−37	37	0.000
- small volume-corrected peak						0.000*
Inferior Parietal Lobule	40	R	57	−43	40	0.000
Superior Frontal Gyrus	6	R	9	14	58	0.001
Superior Frontal Gyrus	6	L	−6	8	58	0.002
vOICe Distract Counting [Post – Pre]						
Inferior Parietal Lobule	40	R	57	−43	40	0.000
- small volume-corrected peak						0.000*
Inferior Parietal Lobule	40	R	51	−34	37	0.002
Postcentral Gyrus	3	L	−21	−34	70	0.002
Star Trek Sound Pause Detection [Post – Pre]						
Inferior Parietal Lobule	40	R	57	−43	40	0.000
- small volume-corrected peak						0.006*
Inferior Parietal Lobule	40	R	48	−34	37	0.001
Beach Sound Pause Detection[Post – Pre]						
Inferior Parietal Lobule	40	R	54	−46	40	0.000
- small volume-corrected peak						0.008*

B

Late Blind Participants (*N* = 1) (RD)						
Region	**BA**	**Side**	***x***	***y***	***z***	p_{uncorr}
vOICe Noise Pause Detection [Post – Pre]						
Inferior Parietal Lobule	40	R	69	−25	25	0.000
- small volume-corrected peak						0.000*
Precentral Gryus	4	R	60	−7	22	0.000
Supermarginal Gyrus	40	R	51	−52	25	0.000
Inferior Parietal Lobule	40	L	−60	−28	28	0.000
Supermarginal Gyrus	40	L	−48	−49	34	0.000
Supermarginal Gyrus	40	L	−42	−37	34	0.000
Middle Temporal Gyrus	39	L	−45	−67	25	0.000
- small volume-corrected peak						0.000*
Caudate		R	21	−1	22	0.000
Caudate		R	18	8	22	0.000
Cingulate Gyrus	24	R	24	−10	34	0.000
Superior Frontal Gyrus	8	R	18	38	52	0.000
Middle Frontal Gyrus	8	R	24	38	40	0.003
Lingual Gyrus	19	R	33	−61	1	0.000
- small volume-corrected peak						0.009*
Caudate		L	−15	8	19	0.000
Caudate		L	−18	−16	22	0.002
vOICe Distract Counting [Post – Pre]						
Middle Temporal Gyrus		R	51	−34	1	0.000
Superior Temporal Gyrus		R	63	−16	−2	0.000
Cuneus	17	R	12	−82	10	0.000
- small volume-corrected peak						0.000*

Late Blind Participants (*N* = 1) (RD) Continued						
Region	**BA**	**Side**	***x***	***y***	***Z***	p_{uncorr}
Posterior Lobe, Cerebellum		R	30	−64	−8	0.000
Posterior Lobe, Cerebellum		R	21	−76	−14	0.000
Insula	13	R	48	−22	25	0.000
Inferior Parietal Lobule	40	R	66	−37	28	0.000
- small volume-corrected peak						0.000*
Inferior Parietal Lobule	40	R	39	−52	43	0.000
Middle Frontal Gyrus	8	L	−33	35	43	0.000
Middle Frontal Gyrus	8	L	−30	26	40	0.000
Middle Frontal Gyrus	9	L	−39	38	34	0.000
Inferior Parietal Lobule	40	L	−54	−28	25	0.000
Insula	13	L	−45	−19	19	0.000
Cingulate Gyrus	32	L	0	17	40	0.000
Medial Frontal Gyrus	6	L	−9	−4	58	0.000
Beach Sound Pause Detection [Post – Pre]						
Precuneus	19	L	−24	−85	43	0.000
- small volume-corrected peak						0.000*
Supramarginal Gyrus	40	L	−60	−46	37	0.000
- small volume-corrected peak						0.000*
Superior Occipital Gyrus	19	L	−36	−82	34	0.000
Middle Temporal Gyrus	39	R	45	−61	28	0.000
- small volume-corrected peak						0.001*
Inferior Parietal Lobule	40	R	69	−25	25	0.000
Precuneus	19	R	33	−79	34	0.000
Middle Frontal Gyrus	8	L	−45	17	49	0.000

Late Blind Participants (*N* = 1) (RD) Continued						
Region	**BA**	**Side**	***x***	***y***	***Z***	p_{uncorr}
Superior Frontal Gyrus	8	L	−27	44	40	0.000
Superior Frontal Gyrus	9	L	−18	59	34	0.005
Superior Frontal Gyrus	9	L	−27	56	34	0.008
Superior Frontal Gyrus	10	L	−42	50	25	0.000
Lingual Gyrus	19	L	−33	−67	−2	0.004
Star Trek Sound Pause Detection [Post – Pre]						
Cuneus	17	R	9	−82	10	0.000
- small volume-corrected peak						0.000*
Lingual Gyrus	18	L	−15	−79	−5	0.000
- small volume-corrected peak						0.003*
Lingual Gyrus	18	R	18	−70	4	0.000
Superior Temporal Gyrus	39	R	48	−55	25	0.000
- small volume-corrected peak						0.000*
Inferior Parietal Lobule	40	R	69	−31	28	0.000
- small volume-corrected peak						0.000*
Postcentral Gyrus	2	R	45	−25	31	0.000
Middle Temporal Gyrus	39	L	−42	−61	25	0.000
Inferior Parietal Lobule	40	L	−57	−28	25	0.000
Inferior Parietal Lobule	40	L	−48	−34	28	0.000
Precuneus	19	R	33	−79	34	0.001
- small volume-corrected peak						0.044*
Precuneus	7	L	−21	−79	49	0.002

C

Congenitally Blind Participants (*N* = 1) (WB)						
Region	**BA**	**Side**	***x***	***y***	***z***	p_{uncorr}
vOICe Noise Pause Detection [Post – Pre]						
No Activation						
vOICe Distract Counting [Post – Pre]						
Insula	13	L	−39	−4	1	0.001
Lentiform Nucleus		L	−21	2	4	0.002
Lentiform Nucleus		L	−30	−1	7	0.003
Posterior Cingulate	30	R	3	−49	19	0.001
Culmen		R	15	−40	−8	0.001
Lingual Gyrus	19	R	15	−49	−2	0.001
- small volume-corrected peak						0.024*
Superior Frontal Gyrus	6	R	12	23	64	0.001
Superior Frontal Gyrus	6	R	9	11	64	0.004
Claustrum		L	−33	−22	4	0.001
Middle Frontal Gyrus	11	L	−36	35	−11	0.003
Culmen		L	−9	−31	−14	0.003
Parahippocampal Gyrus		L	−33	−4	−20	0.005
Star Trek Sound Pause Detection [Post – Pre]						
Subcallosal Gyrus	34	R	12	2	−11	0.001
Subthalamic Nucleus, Midbrain		R	12	−13	−5	0.002
Beach Sound Pause Detection [Post – Pre]						
No Activation						

D

Congenitally Blind Participants (*N* = 1) (SB)						
Region	**BA**	**Side**	***x***	***y***	***z***	p_{uncorr}
vOICe Noise Pause Detection [Post – Pre]						
Inferior Parietal Lobule	40	R	48	−31	25	0.000
- small volume-corrected peak						0.000*
Supramarginal Gyrus	40	L	−42	−37	31	0.000
Cuneus	18	R	3	−97	22	0.000
- small volume-corrected peak						0.000*
Middle Frontal Gyrus	8	L	−42	23	43	0.000
Middle Frontal Gyrus	8	L	−30	35	46	0.000
Superior Frontal Gyrus	6	R	18	29	55	0.000
Superior Parietal Lobule	7	L	−33	−52	64	0.000
Postcentral Gyrus	7	R	9	−49	64	0.006
Cingulate Gyrus	32	L	−21	2	34	0.000
vOICe Distract Counting [Post – Pre]						
Cingulate Gyrus	24	L	0	11	31	0.000
Middle Frontal Gyrus	9	L	−27	20	34	0.001
Insula	13	R	51	−19	22	0.003
Star Trek Sound Pause Detection [Post – Pre]						
Inferior Parietal Lobule	40	L	−42	−34	28	0.000
Insula	13	L	−51	−19	25	0.000
Inferior Parietal Lobule	40	L	−48	−46	40	0.000
Inferior Parietal Lobule	40	R	51	−25	25	0.001
Precuneus	31	L	−15	−43	34	0.001
Beach Sound Pause Detection [Post – Pre]						
Superior Frontal Gyrus	6	L	−18	11	67	0.000
Superior Parietal Lobule	7	L	−27	−58	67	0.000

Congenitally Blind Participants (*N* = 1) (SB) Continued						
Region	**BA**	**Side**	***x***	***y***	***z***	p_{uncorr}
Insula	13	R	48	−25	22	0.001
Postcentral Gyrus	3	L	−45	−19	64	0.001
Inferior Parietal Lobule	40	L	−51	−49	43	0.002
Inferior Parietal Lobule	40	L	−39	−34	31	0.002
Cingulate Gyrus	24	R	3	−10	34	0.003

Table 4.4. fMRI data: Post – pre training blind and severe low-vision participants. Select imaging results for severe low-vision participant ($N = 1$), Panel A, a late blind participant ($N = 1$), Panel B, and two congenitally blind participants ($N = 2$), Panel C and D, when comparing post-vOICe-training scan and the pre-vOICe-training scan. For the late blind participant, only the top 15 clusters of activation are presented in Panel B; a full list is in Appendix D, Table B. All regions were limited to $p < 0.009$ uncorrected and 10 voxel cluster threshold (p_{uncorr} refers to the peak level p_{uncorr}). The small volume correction was for a sphere of 10 millimeter radius around the cluster center, and the pvalue shown (indicated by asterisk, *i.e.*, *) is for the peak level FWE-corrected. Brodmann Area localization was performed on the talaraich client for nearest grey matter. Any clusters without nearest grey matter within +/− 5 mm are not included.

Sighted Participant Covariate Analyses of Imaging Data

Following the final fMRI imaging session, participants filled out a post-experiment questionaire to identify the role of visualization, the completeness of the distraction in the distraction task, and other relevant parameters. This was meant to see whether the subjective post-hoc report of visualization and/or attentiveness was correlated with fMRI activation in the visual cortex. The survey is presented in full in Appendix C. The sighted participant results ($N = 10$) from four of the questions from this questionaire are presented in Figure 4.14. Figure 4.14A shows that the number of sighted participants that recognized the vOICe noise as the vOICe device dramatically increased from the first fMRI session (pre-training) to the second session (post-training). Figure 4.14B shows that most participants in the pre-training and post-training fMRI scans were not distracted from the task of counting by the playing of the vOICe sound in the background. The final two plots, Figure 4.14C and 4.14D, indicate that the number of people imagining numbers in the counting task or visual scenes in the familiar sound pause task did not dramatically change between the pre- and post-training sessions.

The data presented in Figure 4.14 (experiment questionaire) and Figure 4.08 (localization accuracy with training) can be used for fMRI covariate analyses. A covariate analysis (details in methods) determines whether a neural activation correlates across participants with a behavioral metric or the subjective post-hoc reports. The behavioral metrics and subjective post-hoc reports used here will include the visual imaginings during the distraction task to determine whether any of the visual activation in the distraction post-pre anaylsis is due to visualization, and the performance metrics at localization (slope and intercept) to determine whether any vOICe learning correlates with the visual activation in the distraction task. Both of these covariates are designed to narrow down the possible origins of the visual activation in the distraction task, ideally showing that visualization did not play a role, and the vOICe learning did. With this correlative tie between the visual activation in the distraction task and the vOICe learning, it can more postively be stated that crossmodal plasticity with vOICe is automatic (*i.e.,* can occur without attention).

The results for the covariate analysis on the distraction vOICe results are presented in Table 4.5. The first covariate tested was to disprove the visualization hypothesis, that the activation in distraction task was due to visual imaginings of shapes or numbers. The covariate for this analysis was generated from the data in Figure 4.14C by making imagined numbers response = 1, not imagining numbers response = 0, and summing across the pre- and post-training fMRI sessions (*i.e.,* the max number was 2 if participant imagined in both sessions, and the minimum was 0 if the participant imagined in no sessions). The analysis indicates that no neural activation correlated with the imagining number behavioral metric. In addition, the number of participants that imagined numbers decreased from the pre-training to the post-training sessions (Figure 4.14C). Therefore, combining the covariate analysis and the decreasing number of participants with visualization from pre to post, it is unlikely that the visual activation in the distraction counting task was due to visualization.

The visualization covariate result is the most important and valuable to this study. This null result for visualization in the vOICe distraction counting task (Table 4.5) indicates that the visual activation in the distraction task is not likely due to visualization of numbers and shapes. Therefore, the visual activation is likely from crossmodal plasticity engendered automatically from vOICe training. In addition, the visualization covariate result strengthens the case for automatic processing with vOICe in early visual regions of cortex (*i.e.,* BA 18 and 19).

The two other covariates performed on the distraction vOICe [Post – Pre] results used the vOICe training performance at the localization task. It is useful to note that localization performance is not a broad metric of vOICe interpretation ability, nor is the distraction task in fMRI using localization. Therefore, any neural activations that correlate with the vOICe localization covariates may be interesting, but the lack of a correlation between localization performance and visual activation from a vOICe counting distraction task would not diminish the vOICe fMRI results. It is particularly important to be aware of this for the vOICe device, because participants perform at different levels for different vOICe tasks. For example, a participant that is excellent at vOICe localization may be poor at recognition with vOICe. Therefore, for a vOICe performance metric to be a valuable covariate, it should be as close as possible to the vOICe task in the fMRI scanner. Since vOICe localization and the vOICe counting distraction task are not that behaviorally similar, it diminishes the value of this vOICe covariate fMRI result. This qualification to covariate correlation analyses will be revisited in more detail later.

The first vOICe covariate is the performance improvement (slope) for the localization inaccuracy *vs.* training time plot (Figure 4.08 and 4.09). Since the y-axis is a measure of inaccuracy, a smaller slope (*i.e.,* more negative) means a better learning rate. Therefore, the slope of each participants data was multiplied by -1 to invert the data, making the larger slope values represent the best performing participants. This slope covariate generated several neural regions that correlated with the slope (Table 4.5), including BA 6, 8, 24, and 32. These neural regions have been known to be involved with motor functions, auditory imagery, language, memory, executive functions and visuospatial attention. It is likely that these regions engaged in several of these functions during the counting distraction task. This frontal lobe region activation may correlate with participant improvement at the localization task, because participants that improved the most used a cognitive, top-down strategy in learning, therefore engaging pre-frontal regions more vigorously than the participants that did not improve as much. Since improvement (slope) and initial performance (intercept) are anticorrelated (Figure 4.10), it is also conceivable that the participants that did not improve as much were *better at the beginning of training,* and therefore engaged in a more automatic, perceptual strategy (with less frontal neural activity) based on crossmodal correspondences.

The second covariate based on localization vOICe data uses the beginning performance (intercept) of the localization performance *vs.* training time. The localization data is plotted as inaccuracy *vs.* training time (smaller values = more accurate localization). Therefore, to make the largest values the most accurate, all intercept values were mulitplied by -1 (larger values = most accurate). No neural activation correlated with initial performance at vOICe for the [Post – Pre] distract counting task (Table 4.5). It is logical that this would be true, as the contrast compares the post-training scan with the pre-training scan, therefore identifying the changes due to training, whereas the covariate is for the initial performance and not training changes. While this covariate is less valuable to the vOICe distraction [Post – Pre] contrast, it will be more relevant when used with later contrasts in Chapter 5 that compare tasks within one fMRI session (*i.e.* only before training, or only after training).

A

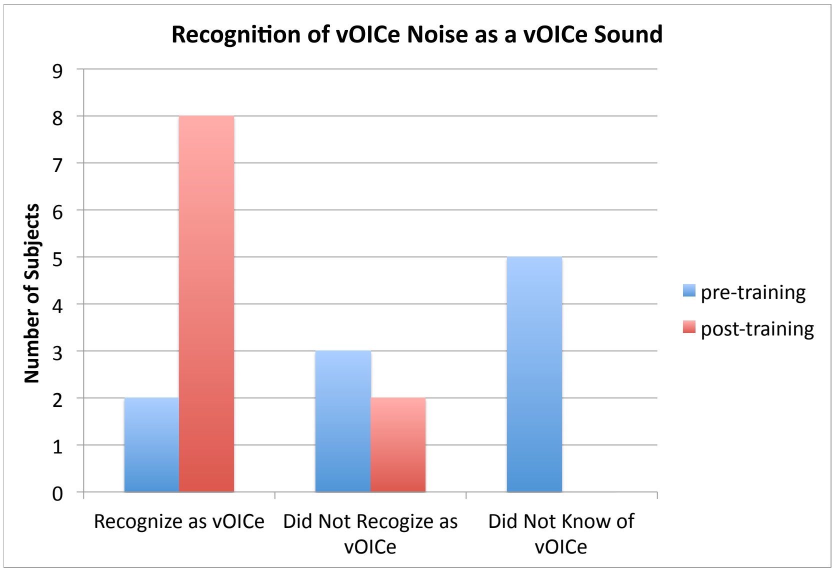
Recognition of vOICe Noise as a vOICe Sound
Number of Subjects
9
8
7
6
5
4
3
2
1
0
Recognize as vOICe
Did Not Recogize as vOICe
Did Not Know of vOICe
pre-training
post-training

B

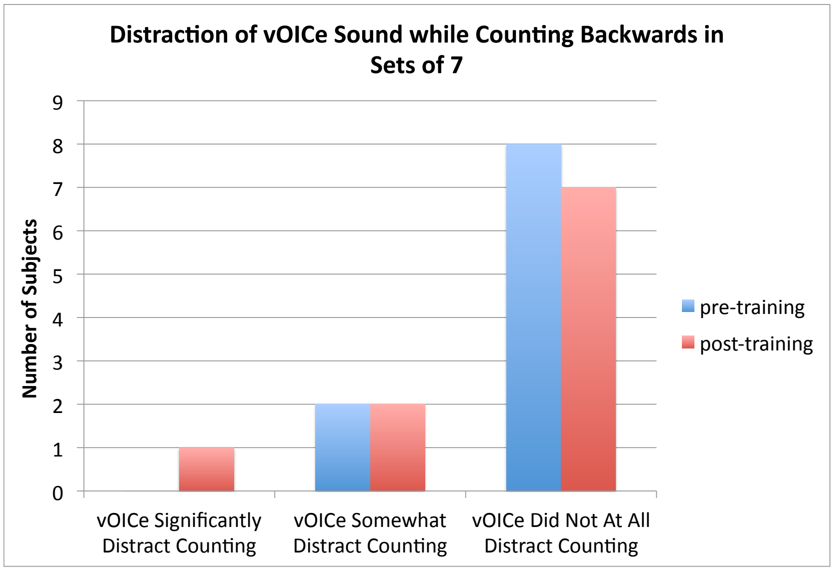
Distraction of vOICe Sound while Counting Backwards in Sets of 7
Number of Subjects
9
8
7
6
5
4
3
2
1
0
vOICe Significantly Distract Counting
vOICe Somewhat Distract Counting
vOICe Did Not At All Distract Counting
pre-training
post-training

C

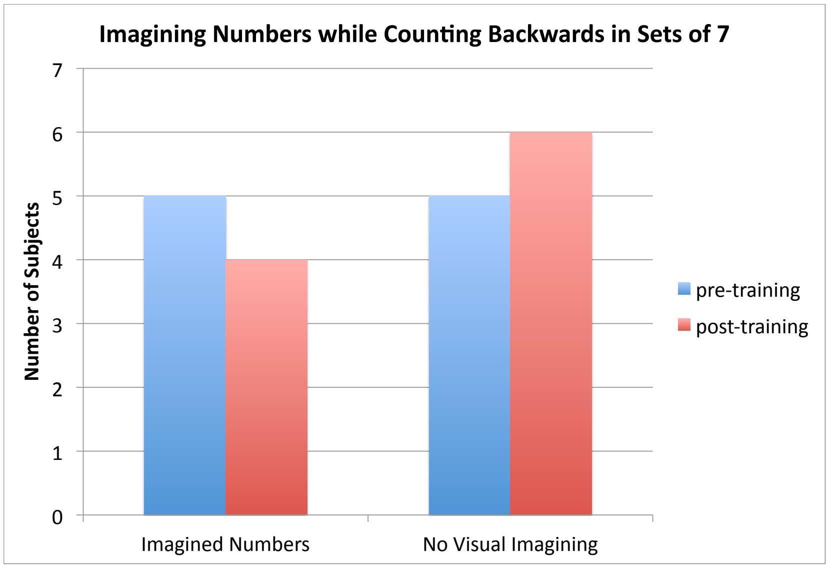

D

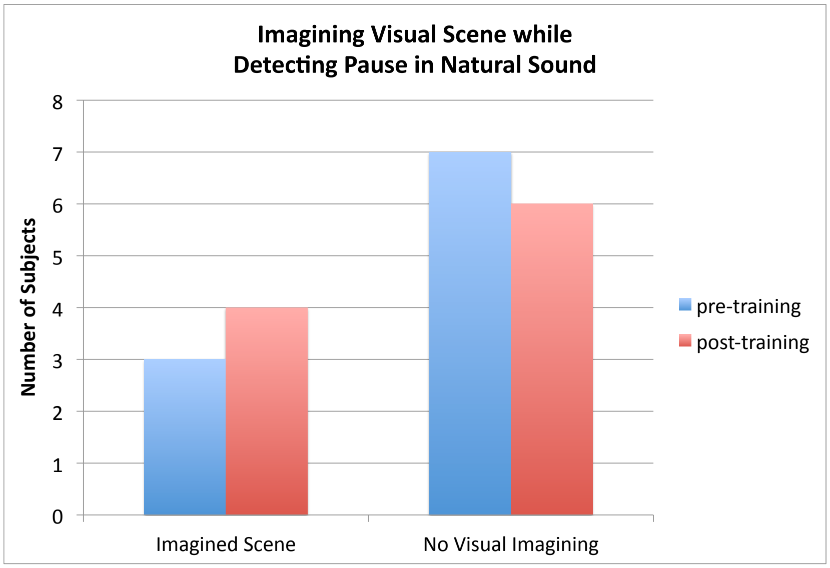

Figure 4.14. Post-experiment Questionaire Results. Following the post-training fMRI scan, all participants filled out a questionaire (Appendix C). This figure plots the responses to select questions in that questionaire for the 10 sighted participants.

Sighted Participants ($N = 10$)						
Region	BA	Side	x	y	z	p_{uncorr}
Distract Counting [Post – Pre] Visualization Covariate						
No Activation						
Distract Counting [Post – Pre] Localization Slope Covariate						
Sub-Gyral	6	L	−15	−4	52	0.001
Cingulate Gyrus	24	L	−15	−4	43	0.001
Middle Frontal Gyrus	6	L	−30	−10	43	0.001
Superior Frontal Gyrus	8	R	21	26	46	0.001
Medial Frontal Gyrus	6	L	−9	−25	67	0.001
Medial Frontal Gyrus	6	R	6	−25	67	0.003
Medial Frontal Gyrus	32	R	6	8	46	0.003
Medial Frontal Gyrus	6	L	0	−4	49	0.003
Distract Counting [Post – Pre] Localization Intercept Covariate						
No Activation						

Table 4.5. fMRI covariate data: Post – pre training vOICe noise distract sighted participants. Three covariates for vOICe Noise Distract task are displayed in this table: one for visualization, and two based on vOICe training performance. Details on the processing of covariates is in the methods section and the results section of Chapter 4. The neural activation shown for vOICe Noise Distract [Post – Pre] correlates with the performance of the covariate listed, indicating that the covariate may have played a role in generating the neural activation listed. All regions were limited to $p < 0.009$ uncorrected and 10 voxel cluster threshold. Brodmann Area localization was performed

on the talaraich client for nearest grey matter. Any clusters without nearest grey matter within +/– 5 mm are not included.

Sighted Participant Visual Suppression Following vOICe Training

All previous Chapter 4 fMRI contrasts have investigated the impact of vOICe training on crossmodal interaction and plasticity. The results of these contrasts indicated that in the sighted participants (*N* = 10), the severely impaired (*N* = 1), and most blind participants (*N* = 2) there was automatic activation of multimodal or visual regions to vOICe stimuli. It is also interesting to investigate whether this crossmodal plasticity had an impact on traditional visual perception in the sighted participants. It is possible that the vOICe-based new crossmodal connectivity enhances the effectiveness of processing in the visual cortex. In particular, the blindfolding of sighted individuals has been known to increase visual region excitability (Boroojerdi et al., 2000). As the sighted participants were blindfolded for 5 hours during our vOICe training, this is a possible outcome. However, it may also be possible, as an alternative, that auditory (or crossmodal) connections to visual cortex are in competition with visual connections to visual cortex. Therefore, when the crossmodal influence on visual cortex is increased by the vOICe training, the visual dominance of visual cortex may be slightly weakened. In support of this hypothesis, a study by Rauschecker and Korte used visual deprivation on cats to induce neuron sensitivity to auditory stimuli and to decrease sensitivity to visual stimuli in the anterior ectosylvian (AE) cortex known for visual processing alone (Rauschecker & Korte, 1993). They conjectured that because the visual response was reduced when the crossmodal activations of AE were increased, that the two types of input were in competition for dominance.

We tested for this suppression or strengthening of visual activation of visual cortex with a simple visual task performed before and after vOICe training in sighted participants. Participants were asked to view a white noise visual image and detect whether it paused during its presentation, and then respond with a button press. The imaging contrast of this task (vision noise pause detection) was activation following vOICe training subtracted from activation before vOICe training to determine whether any visual regions were less active after the vOICe training compared to before (Table 4.6 and Figure 4.15). The results indicate that several visual and multisensory regions' (such as BA 19, and 40) activity were suppressed significantly following the vOICe training. These regions of visual suppression are similar to the regions crossmodally activated by vOICe stimuli in the same sighted participants (Table 4.1 and 4.2) and in the blind participants (Table 4.4). In other words, two processes (visual and crossmodal) are likely competing for the activation of same visual and multimodal regions; as crossmodal plasticity is strengthened (as seen in the vOICe tasks), traditional vision is weakened (as seen in the visual noise task).

It is important to control for the possibility that not visual suppression but rather fatigue or inattention is causing a reduction in visual activation following vOICe training. Certainly neural fatique or diminished interest could also cause a decrease in visual activation in the second session (following vOICe training) in comparison to the first session (before vOICe training). To control for these possibilities, we used a covariate of performance of participants during vOICe training to determine whether any regions of suppression correlated with the vOICe performance. If suppression in the regions of interest correlate with vOICe performance, then that would indicate that the suppression is likely tied to vOICe training rather than other spurious factors.

The first vOICe performance covariate tested is the amount of improvement at the localization task (Figure 4.08) or the negative of the slope in the localization inaccuracy curve (covariate detailed in methods p. 144, and in previous section p. 178-186). No regions of neural activation for vision noise pause detection [Pre – Post] correlated with the vOICe improvement covariate.

The second covariate is the initial performance at the vOICe localization task (Figure 4.08), or the negative of the y-intercept in the localization inaccuracy curve (covariate detailed in methods p. 144, and in previous section p. 178-186). Many visual and multimodal regions that were similar to the regions of visual suppression in the vision noise contrast, did indeed correlate with this second initial vOICe performance covariate (BA 40, 17, and 18; BA 17 is significant with small volume correction; Table 4.7). Therefore, this result means that the visual and multimodal suppression is likely tied to the vOICe training between the sessions rather than changes in arousal or neural fatigue. The initial performance correlation with visual suppression may demonstrate that the initial individual crossmodal strength plays an important role in shaping the neural dynamics of crossmodal plasticity, and therefore visual suppression. Improvement at the vOICe task may be less useful than the initial performance as a covariate with visual suppression, because improvement at localization with vOICe is limited by the performance ceiling, whereas initial performance is not.

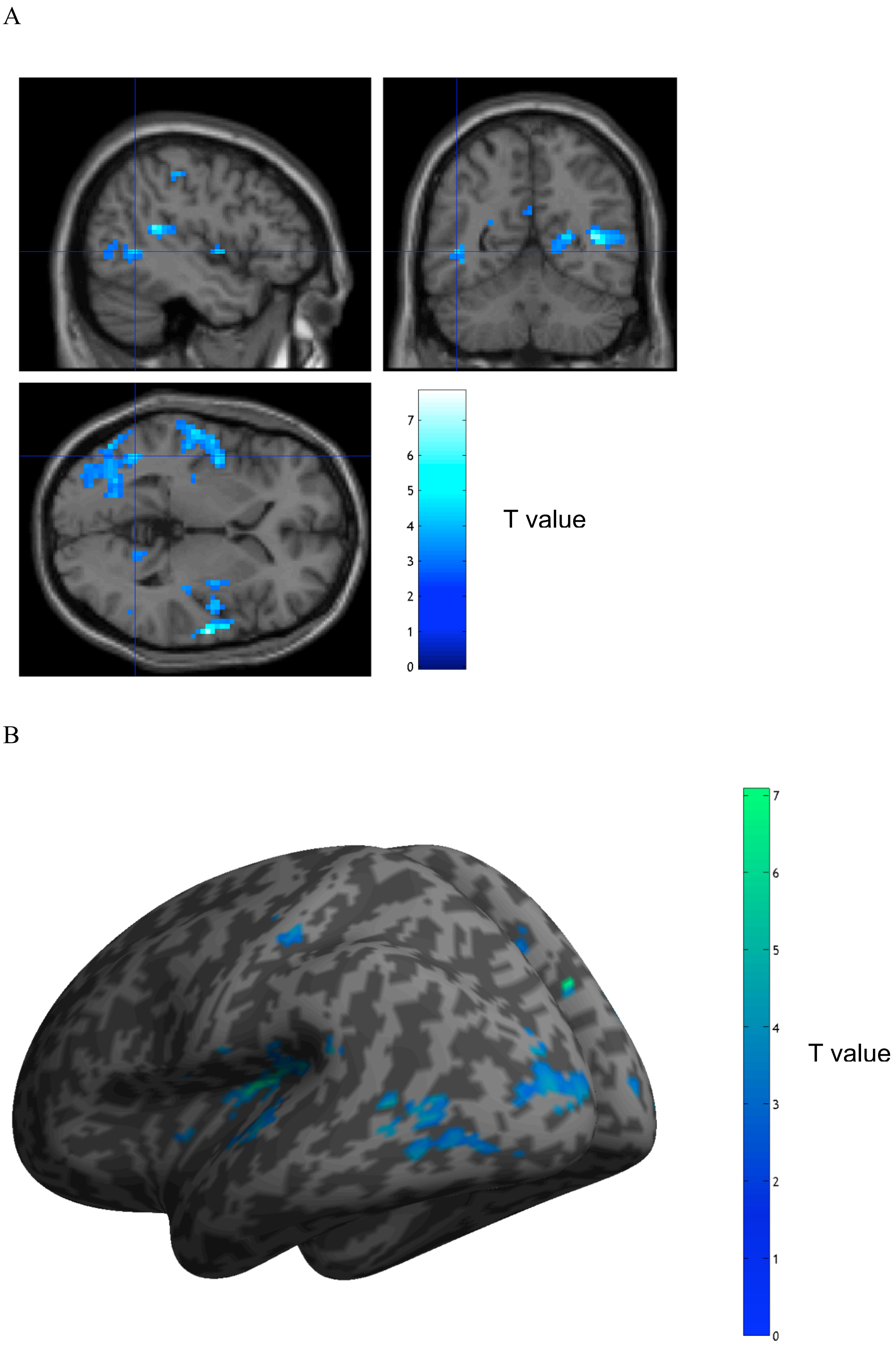
A
7
6
5
4
3
2
1
0
T value
B
7
6
5
4
3
2
1
0
T value

Figure 4.15. fMRI data: Pre – post training vision noise pause detection task in sighted participants. The neural imaging result is displayed for pre-vOICe-training in contrast to post-vOICe-training for the vision-noise pause detection task in sighted participants ($N = 10$). Imaging data presented is $p < 0.009$ uncorrected and clusters of 10 voxels or more; further correction for multiple comparisons is shown in Table 4.6. Methods for fMRI data display are in the Chapter 4 methods. Activation is shown in blue to indicate that activation with a [Pre – Post] contrast is in fact representing a suppression of activation if the typical [Post – Pre] contrast was used (as was used in all other contrasts in Chapter 4). Therefore, relative to all other Chapter 4 figures, which present visual activation, Figure 4.15 represents visual suppression. The detailed description of methods for fMRI data display are in the Chapter 4 methods.

Sighted Participants (*N* = 10)						
Region	BA	Side	*x*	*y*	*z*	p_{uncorr}
Vision Noise Pause Detection [Pre – Post]						
Superior Temporal Gyrus	22	R	66	−10	4	0.000
Insula	13	R	36	−19	19	0.000
Precentral Gyrus	6	R	54	−1	13	0.000
Superior Temporal Gyrus	13	L	−42	−43	16	0.000
Insula	13	L	−30	−28	16	0.000
Superior Temporal Gyrus		L	−60	−19	1	0.001
Precuneus	7	R	21	−70	31	0.000
Superior Temporal Gyrus	22	R	39	−55	10	0.000
Posterior Cingulate	30	R	27	−70	13	0.000
Superior Temporal Gyrus	22	L	−63	−46	19	0.000
Inferior Parietal Lobule	40	R	57	−31	46	0.000
- small volume-corrected peak						0.020*
Precentral Gyrus	4	R	51	−7	46	0.001
Postcentral Gyrus	2	R	54	−25	55	0.001
Paracentral Lobule	31	R	9	−10	43	0.000
Paracentral Lobule	31	L	0	−10	46	0.001
Cingulate Gyrus	24	R	9	−1	46	0.002
Precuneus	31	L	−3	−61	28	0.001
Posterior Cingulate	23	L	0	−46	25	0.006
Inferior Temporal Gyrus	19	L	−45	−55	1	0.001
- small volume-corrected peak						0.035*
Middle Occipital Gyrus	19	L	−30	−88	10	0.001
Lingual Gyrus		L	−30	−73	4	0.001
Inferior Parietal Lobule	40	L	−48	−28	49	0.001

Sighted Participants (*N* = 10) Continued						
Region	BA	Side	x	y	z	p_{uncorr}
Superior Temporal Gyrus	22	R	48	−7	1	0.002
Precuneus	31	L	−18	−73	28	0.002
Cuneus	18	L	−12	−76	22	0.002
- small volume-corrected peak						0.076*
Precuneus	7	R	9	−67	43	0.003

Table 4.6. fMRI data: sighted participants' vision noise pause detection [Pre – Post]. Imaging results for sighted participants ($N = 10$) when comparing pre-vOICe-training scan and the post-vOICe-training scan for visual noise pause detection task. All regions were limited to $p < 0.009$ uncorrected and 10 voxel cluster threshold (p_{uncorr} refers to the peak level p_{uncorr}). The small volume correction was for a sphere of 10 millimeter radius around the cluster center, and the pvalue shown (indicated by asterisk, *i.e.*, *) is for the peak level FWE-corrected. Brodmann Area localization was performed on the talaraich client for nearest grey matter. Any clusters without nearest grey matter within +/− 5 mm are not included.

Sighted Participants (*N* = 10)						
Region	BA	Side	*x*	*y*	*z*	p_{uncorr}
Vision Noise Pause Detection [Pre – Post] Localization Slope Covariate						
No Activation						
Vision Noise Pause Detection [Pre – Post] Localization Intercept Covariate						
Insula	13	R	39	−13	13	0.000
Superior Temporal Gyrus	22	R	51	−10	1	0.000
Superior Temporal Gyrus	22	R	57	−1	1	0.001
Superior Temporal Gyrus	22	R	60	−34	13	0.000
Superior Temporal Gyrus	41	R	48	−31	13	0.000
Inferior Parietal Lobule	40	R	69	−37	28	0.001
- small volume-corrected peak						0.064*
Superior Temporal Gyrus	41	L	−48	−34	10	0.000
Superior Temporal Gyrus	22	L	−45	−28	1	0.001
Superior Frontal Gyrus	6	L	0	11	67	0.000
Superior Frontal Gyrus	6	R	9	5	67	0.003
Superior Temporal Gyrus	41	L	−57	−19	4	0.000
Transverse Temporal Gyrus	42	L	−63	−16	10	0.001
Cuneus	17	L	−12	−94	4	0.000
- small volume-corrected peak						0.029*
Thalamus, Pulvinar		R	15	−28	10	0.003
Superior Frontal Gyrus	6	L	−21	−1	67	0.001
Cuneus	17	R	18	−82	7	0.002
Middle Occipital Gyrus	18	R	30	−79	4	0.008
- small volume-corrected peak						0.167*

Table 4.7. fMRI covariate data: Pre – post training vision noise in sighted participants. Two covariates for the vision noise pause task are displayed in this table; both are based

on vOICe training performance. Details on the processing of covariates is in the methods section and the results section of Chapter 4. The neural activation shown for vision noise pause detection [Pre – Post] correlates with the performance of the covariate listed, indicating that the covariate may have played a role in generating the neural activation listed. All regions were limited to $p < 0.009$ uncorrected and 10 voxel cluster threshold. The small volume correction was for a sphere of 10 millimeter radius around the cluster center, and the pvalue shown (indicated by asterisk, *i.e.*, *) is for the peak level FWE-corrected. Brodmann Area localization was performed on the talaraich client for nearest grey matter. Any clusters without nearest grey matter within +/– 5 mm are not included

Discussion

Sensory substitution interpretation and neural processing has been presumed to be serial, cognitive, and not automatic (detailed in Chapter 1). This fMRI study of the automaticity of sensory substitution neural activation has dramatically altered this top-down theory of sensory substitution processing. Our results indicate that sensory subsitution can be processed in visual cortical regions without attention or image structure (*i.e.,* white noise image used) in sighted and blind vOICe users. Imaging correlations with participant post-hoc reports show that automatic visual activation from vOICe (*i.e.* during a distraction task) is not likely due to visualization. Further, an interesting result of visual suppression during a visual pause detection task when comparing post-vOICe-training to pre-vOICe-training indicates that crossmodal and natural visual processing may be in competition for dominance in visual cortical regions.

vOICe in Comparison to Vision

The passive processing of sensory substitution in visual regions is similar to visual processing, which can occur at a diminished intensity for unattented objects (for details, see the beginning of Chapter 4). The identification of similarities between sensory substitution (SS) and vision has grown in recent years with the renewed interest in SS's potential. The similarities now include: Functional activation of visual regions (*i.e.,* activation of the FFA while recognizing faces), depth perception, recognition, constancies (detailed in Chapter 2), and causal activation of visual regions by SS (detailed in Chapter 1). The automatic activation of visual cortex can now be added to that list of similarities between SS and vision. Further, the identification of automatic visual processing of SS in visual neural regions indicates that there is automatic perceptual processing of SS that may generate faster training and easier perceptual use. Perhaps the crossmodal mappings discussed in Chapter 3 are one way to tap into this automatic perceptual neural processing of SS.

Prism Adaptation and vOICe Learning

Studies focused on learning new hand-eye relationships via prisms indicate a similar learning pattern to the vOICe localization learning shown in this Chapter. When participants begin using the prism glasses with a shifted or rotated visual transformation, their performance deteriorates due to the inaccuracy of their existing perceptual processing in relation to rotated or shifted vision (Harris, 1965; Shimojo & Nakajima, 1981; von Helmholtz, 1925). However, as the participants use the glasses, their localization and reach and grasp performance gradually improves. Occasionally, the visual perception with prism glasses alters neural processing such that participants no longer visually perceive the shift or rotation from the glasses, indicating adaptive perceptual changes following sensory-motor adaptation (although not all experiments report this perceptual change) (Linden, Kallenbach, Heinecke, Singer, & Goebel, 1999). Both of these patterns occur with vOICe perception; when participants start using the new auditory-visual encoding and camera, their performance is not near the optimal localization performance. Yet, as shown in Figure 4.08 and Figure 4.09, the performance improves to a ceiling based on the systems resolution and the hand-camera coordination. Although not shown in this study, other sensory substitution studies indicate that some blind users have a similar alteration in visual perception to the prism users. In particular, as detailed in Chapter 1, Ortiz *et al.* found that a fraction of blind participants trained on a sensory substitution device also had visual experiences of stimuli perceived with the device (Ortiz, et al., 2011). Further, other expert blind participants have claimed to perceive extensive visual experiences with sensory substitution (Ward & Meijer, 2010) (for details, see Chapter 1). It makes sense that prism learning and SS learning would have these commonalities, as both are the learning of a new hand-eye (or camera) coordination as well as a new transformation algorithm (prism = shift or rotation in vision, sensory substitution = audition to vision). In general, both learning patterns are due to plasticity that adapts to the new unexpected changes in perception, enabling functional learning and rehabilitation.

Automatic vs. Cognitively Demanding Crossmodal Plasticity

It is also interesting to discuss whether the neural activation from perceptual processing of sensory substitution after training uses the same crossmodal interactions as the plasticity evident during demanding cognitive tasks with sensory substitution. As discussed in Chapter 1 and Chapter 3, several crossmodal connections exist before SS training, such as crossmodal correspondences or the connections generating the double flash illusion. These crossmodal interactions can generate visual activation in response to auditory stimulation (detailed in Chapter 1), and may be occuring via direct connections between visual and auditory regions or through indirect feedback connections. Crossmodal plasticity generated by sensory substitution can use these existing connections and modulate their strengths or create new connections. Alternatively, the SS's crossmodal interaction could be ocurring in a multimodal region such as the superior temporal sulcus or the angular gyrus (Beauchamp, Argall, Bodurka, Duyn, & Martin, 2004; Beauchamp, Lee, Argall, & Martin, 2004; Ramachandran & Hubbard, 2003; Spence, 2011). Current cognitively-demanding sensory substitution crossmodal plasticity has been postulated to occur through a top-down (feedback) neural network that includes primary sensory regions as well as multisensory cortical areas (Chapter 1, Figure 1.8). Which feedback neural network or feedforward connections are used is an open question for both the automatic and cognitively-demanding SS plasticity. For detailed comparisons of neural network architectures, DCM modeling of sensory substitution fMRI data is required (DCM details on p. 45). In the meantime, the close correspondence of the neural imaging results (early visual activation) in the automatic task (*i.e.* vOICe distract counting task) and other cognitively demanding tasks in the literature indicate that their neural networks likely have some similarities.